REPORT DOCUMENTATION PAGE

Form Approved
OMB No. 0704-0188

1. AGENCY USE ONLY (Leave blank)	2. REPORT DATE	3. REPORT TYPE AND DATES COVERED
	August 14, 1995	Annual, 1/15 -- 8/15/95

4. TITLE AND SUBTITLE
Coupled Oscillator Control of a Dynamic Four-Legged Robot

5. FUNDING NUMBERS
N00014-95-1-0560

6. AUTHOR(S)
Matthew D. Berkemeier

7. PERFORMING ORGANIZATION NAME(S) AND ADDRESS(ES)
Dept. of Aerospace & Mechanical Engineering
110 Cummington St.
Boston University
Boston, MA 02215

8. PERFORMING ORGANIZATION REPORT NUMBER

9. SPONSORING/MONITORING AGENCY NAME(S) AND ADDRESS(ES)
Office of Naval Research
Ballston Tower One
800 N. Quincy St.
Arlington, VA 22217-5660

10. SPONSORING/MONITORING AGENCY REPORT NUMBER

11. SUPPLEMENTARY NOTES

12a. DISTRIBUTION/AVAILABILITY STATEMENT
Approved for public release;
distribution is unlimited

12b. DISTRIBUTION CODE

13. ABSTRACT (Maximum 200 words)

This report documents progress on a dynamic four-legged robot. After the first seven months of support, we have accomplished the following: 1) We have shown analytically that a platform supported by four springy legs and actuated according to a specific "reflex function" will tend toward motions corresponding to four-legged animal gaits, specifically, the pronk, bound, pace, and rotary gallop. This should greatly simplify legged robot control since the implication is that it is not necessary to pre-program desired behavior such as leg sequences for different gaits. We believe this may also help explain why running animals have chosen particular gaits. 2) We have designed and constructed a leg for our quadrupedal robot which utilizes elastic energy storage to provide most of the force for vertical oscillations. This leg is "biologically-styled" in that elastic tendons drive a rotating foot. Preliminary experimental results have been favorable, and with minor mechanical improvements, we expect to have the leg hopping. Our design was inspired by four-legged animal legs and will give us the opportunity to compare a man-made and biological system at a fairly

14. SUBJECT TERMS (cont.) good level of detail.
Robotics Robot Control Coupled Oscillators
Legged Robots Legged Locomotion

15. NUMBER OF PAGES
12

16. PRICE CODE

17. SECURITY CLASSIFICATION OF REPORT	18. SECURITY CLASSIFICATION OF THIS PAGE	19. SECURITY CLASSIFICATION OF ABSTRACT	20. LIMITATION OF ABSTRACT
Unclassified	Unclassified	Unclassified	

ONR Annual Report

Coupled Oscillator Control of a Dynamic Four-Legged Robot

Grant No. N00014-95-0560
January 15, 1995 – August 15, 1995 (incl. pre-award period)

Principal Investigator:
Prof. Matthew D. Berkemeier
Department of Aerospace and Mechanical Engineering
Boston University
Boston, Massachusetts 02215

1 Overview of Scientific Progress

After seven months of support (incl. pre-award period), we have accomplished the following:

- We have shown analytically that a platform with four springy legs and reflex-like local feedback can have stable oscillatory modes corresponding to gaits of four-legged animals.
- We have designed and built a "biologically-styled" robot leg.
- We have designed and built a leg testing system and have obtained promising preliminary experimental results for our robot leg.

2 Significant Accomplishments

2.1 Analytical Verification of Natural Modes Corresponding to Quadrupedal Gaits in a Mechanical System

Description

Consider a rigid body with springs attached at each corner. The springs are also fixed to the ground. Assume, in addition, that there are sensors at each corner which measure the corner's height, and there are mechanical actuators connected in parallel with the springs which can generate a commanded force. Such a system is a very crude model of a four-legged robot or animal with each spring, sensor, and actuator triple representing a leg. The sensor corresponds to position sensing in the animal leg (muscle spindle organs), the spring corresponds to elastic energy storage (tendons), and the actuator corresponds to force generation (muscles). We chose this system as a first step in modelling four-legged robot/animal dynamics. Our goal was to determine whether, with suitable local feedback corresponding to reflexes, gait-like motions existed. Our focus was on "running-in-place motions," i.e., vertical oscillations without horizontal movements.

Next, we assumed a particular "reflex function" by which we mean a mathematical relationship between sensor output and actutator force. The reflex functions for each leg were identical but completely independent of one another. They were chosen so that energy was added to the system when oscillations were small but removed when oscillations were large. Through application of classical averaging, the coupling of the legs through the body was shown to produce distinct oscillation patterns for the corners. In particular, patterns corresponding to the pronk, bound, pace, and rotary gallop existed and were stable (bound, pace, and rotary gallop were actually only marginally stable).

Finally, oscillatory signals similar to what might be produced by a coupled oscillator controller were introduced and were shown to stabilize the marginally stable gait motions and allow desired transitions between gaits.

Significance

We have shown analytically that a simple system with simple, local feedback, naturally tends to behave in a way that corresponds to animals in nature. This has implications both for legged robot control and for understanding animal locomotion. For legged robot control, this means that it is not necessary to pre-program desired behavior such as leg sequences for different gaits. With simple local feedback, the system will naturally tend toward gait-like motions. This approach is very efficient since little actuator force is required. We believe this may also help explain why running animals have chosen particular gaits; the animals may simply be exploiting natural oscillatory modes that result when simple local reflexes are active within each leg.

Reference

Matthew D. Berkemeier, "Coupled Oscillations in a Platform with Four Springy Legs and Local Feedback," to appear in *Proceedings of the 34th IEEE Conference on Decision and*

Control, New Orleans, Louisiana, December 13–15, 1995. Also available as Boston University, Dept. of Aerospace and Mechanical Engineering Technical Report no. AM-95-009.

Four-Legged Robot/Animal Dynamics

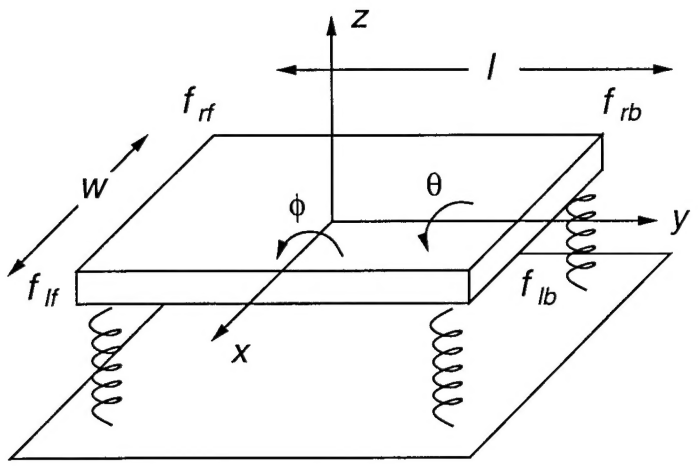

- Spring, actuator, and sensor at each corner.
- Local feedback for each leg.
- Stable motions include only pronk, bound, pace, and rotary gallop.
- Provides control method for robot and may explain animal gait choices.

Convergence to Pronk

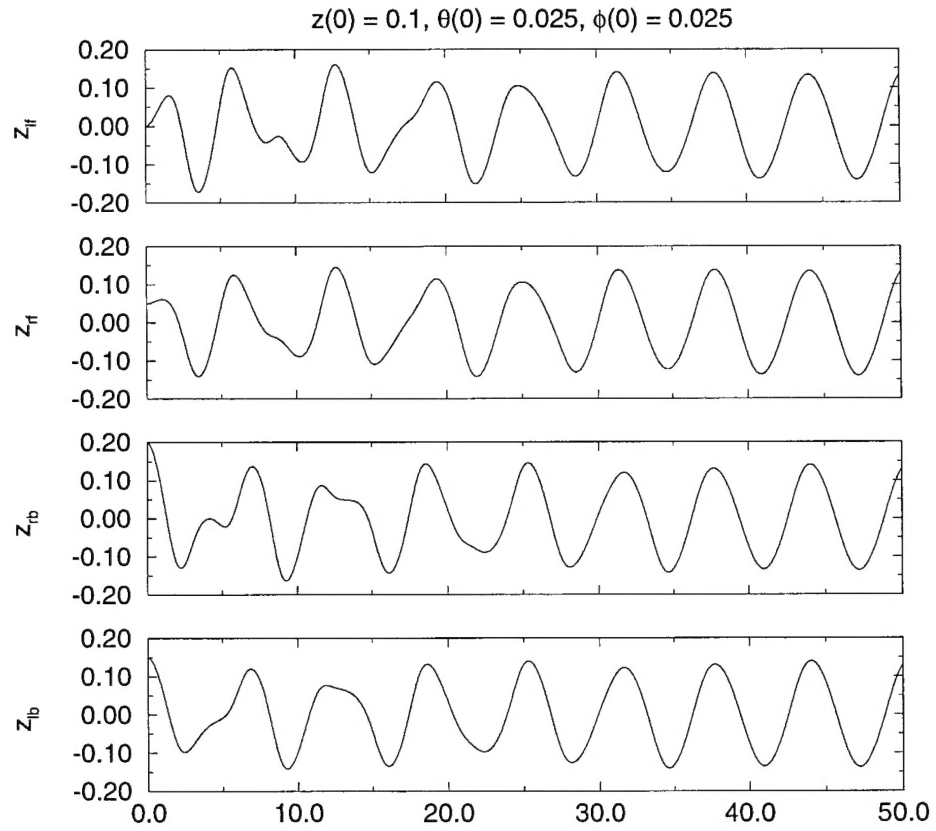

Figure 1: Oscillations of Platform Corners.

Forced Transition from Pronk to Bound

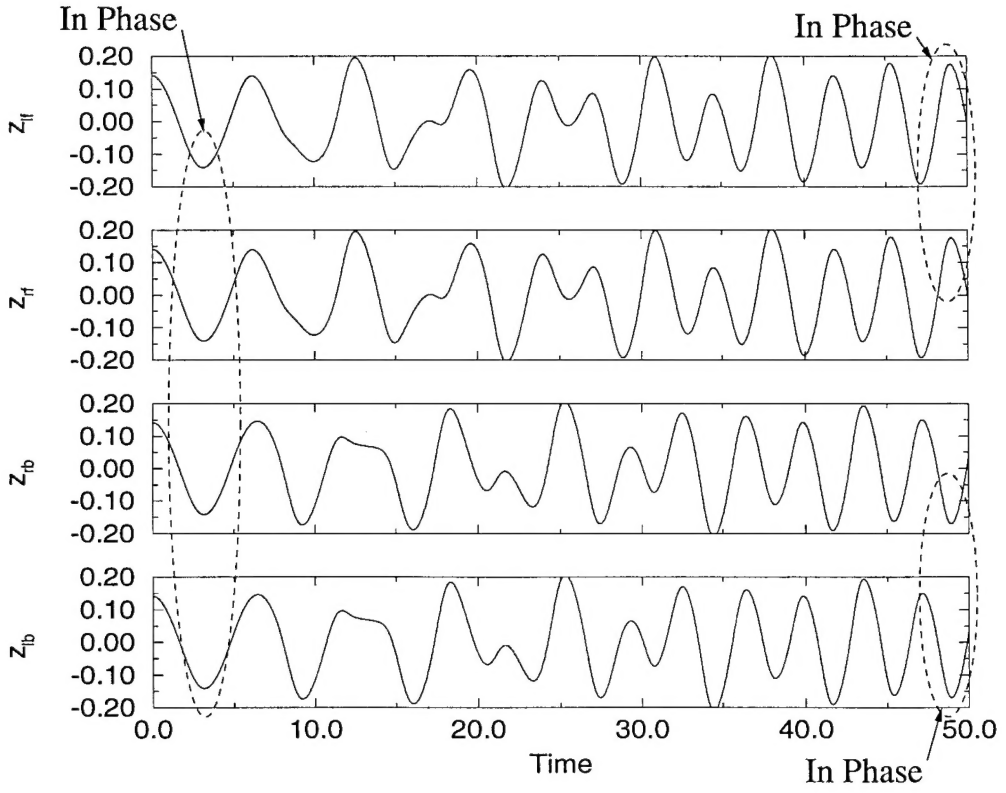

Figure 2: Oscillations of Platform Corners

2.2 Design, Construction, and Testing of a Quadruped Leg

Description

Both biomechanists and roboticists have found that for running gaits, simple leg models consisting of masses and springs are of great utility in understanding (in the biomechanist's case) and controlling (in the roboticist's case) the leg motion. Based on this observation we have used a simple spring and mass leg model to design a novel "biologically-styled" quadrupedal robot leg. It is biologically-styled in that elastic tendons store and release energy to rotate a foot, just like in animals. We have constructed the leg out of aluminum with a DC motor to act as an actuator.

We have also constructed a leg testing system so that we can optimize our leg design without having to build the complete robot. This system consists of an instrumented boom to which our leg prototypes can be attached. We have tested our leg on this system by simply driving the leg at the expected resonance frequency. Results thus far have been encouraging: The ratio of output to input amplitudes was measured to be 4.4 demonstrating the energy conserving nature of the system. With a few mechanical improvements we believe the leg will easily be able to hop.

Other current work on this leg involves comparing key parameter values to those in the cat hindlimb. We hope this will lead to improvements in our design and an increased understanding of the biological system.

Significance

We believe that no one has ever before tested a robot leg with a rotating foot driven by elastic tendons. We have been able to make this leg function in a very short period of time, suggesting that we have a good design. Our design was inspired by four-legged animal legs and will give us a unique opportunity to compare the performance of a man-made and biological system at a fairly good level of detail. This should provide information to both the engineer and the biologist.

Reference

Matthew D. Berkemeier and Kamal V. Desai, "Design of a Robot Leg with Elastic Energy Storage, Comparison to Biology, and Preliminary Experimental Results," planned submission to the 1996 IEEE International Conference on Robotics and Automation and planned Boston University, Dept. of Aerospace and Mechanical Engineering Technical Report.

A Quadrupedal Robot Leg

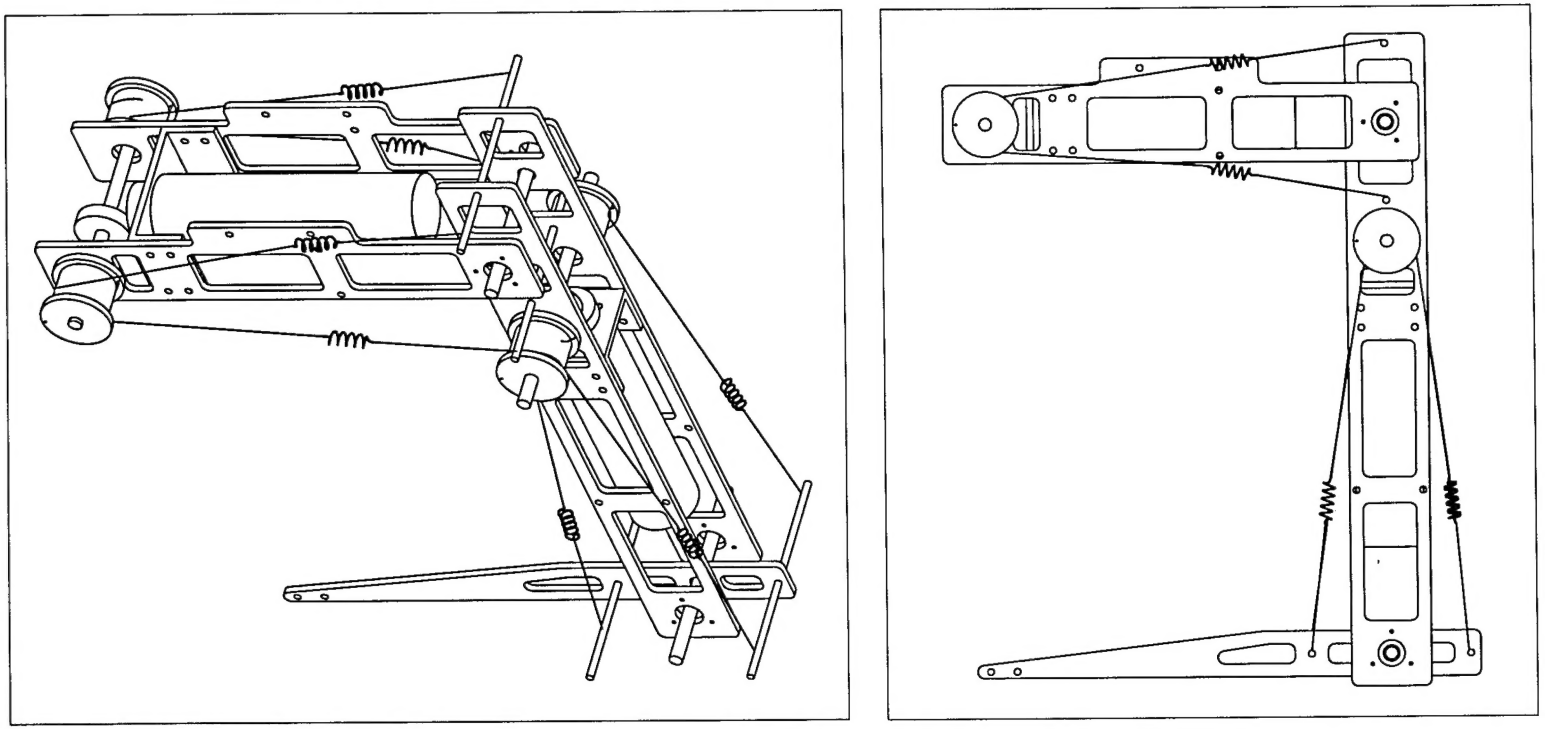

Figure 3: Biologically-Styled Leg Design Includes a Rotating Foot and Elastic Tendons. Leg is 32 cm tall.

Preliminary Experimental Results

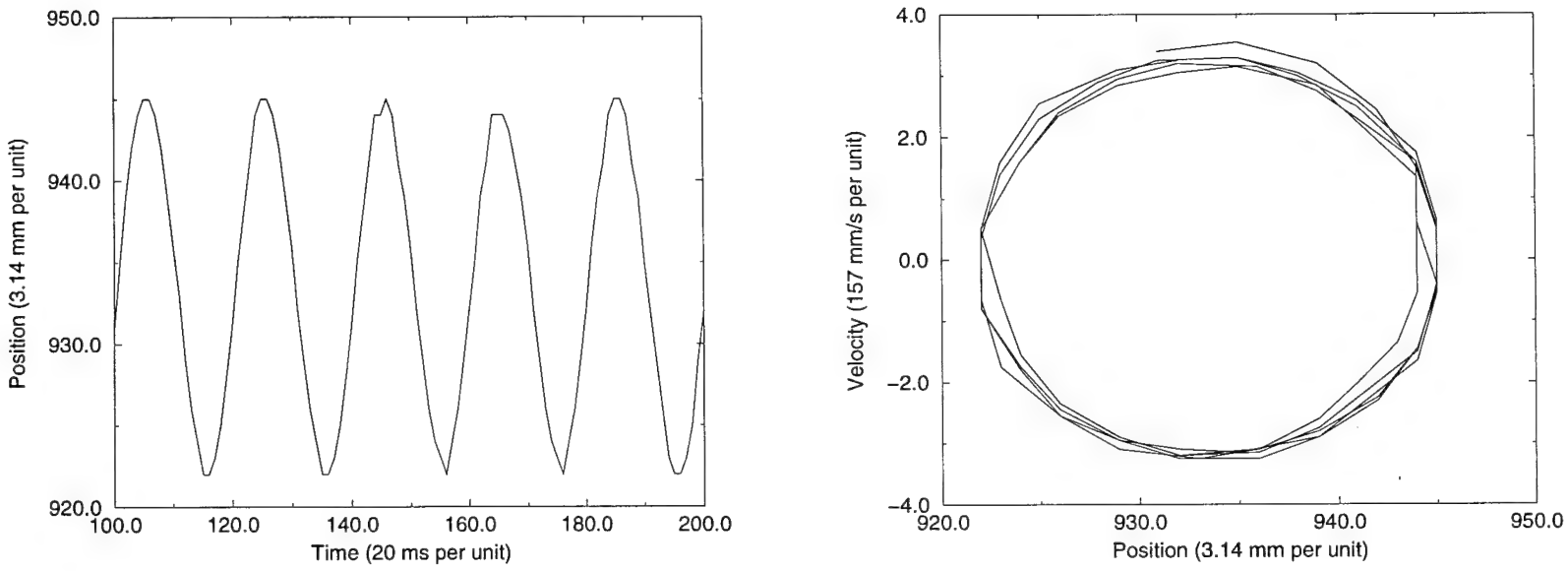

Figure 4: Leg Height Oscillations. Ratio of output to input amplitudes was 4.4 showing energy conservation.

3 Productivity Report

a. Papers Published in Refereed Journals
(none)

b. Papers Accepted for Publication in Refereed Journals
(none)

c. Technical Reports
Matthew D. Berkemeier, "Coupled Oscillations in a Platform with Four Springy Legs and Local Feedback," Boston University, Dept. of Aerospace and Mechanical Engineering Technical Report no. AM-95-009.

d. Books or Book Chapters Published
(none)

e. Books or Book Chapters in Press
(none)

f. ONR-Supported Patents Filed or Granted
(none)

g. Invited Presentations
Matthew D. Berkemeier, "Coupled Oscillations in a Platform with Four Springy Legs and Local Feedback," 34th IEEE Conference on Decision and Control, New Orleans, Louisiana, December 13–15, 1995.

h. Transitions to Industry, Military laboratories or Military Application
(none)

i. Training Data

- Undergraduates: 1 (1 non-US citizen)
- Graduate Students: 1 (1 non-US citizen)

j. Awards/Honors
(none)

k. Number, Cost, and Description of Equipment Items Costing More than $1000

Number	Description	Cost
1	HP 54601B Oscilloscope	$2396
1	HP 33120A Function Generator	$1356
1	Mechanical Dynamics ADAMS Software	$2000

Coupled Oscillations in a Platform with Four Springy Legs and Local Feedback[1]

Matthew D. Berkemeier

March, 1995

Technical Report No. AM-95-009

[1]supported by ONR grant no. N00014-95-1-0560.

Abstract

Research on artificial legged locomotion has the potential for producing vehicles and mobile robots which are capable of easily crossing rocky terrain, climbing or jumping over large obstacles, and agilely maneuvering in tight surroundings. One stumbling block to achieving effective legged robot control is the fact that the problem does not seem to fit well into the framework of modern nonlinear control theory. However, recent results in the modeling of animal central pattern generators by networks of coupled oscillators suggests some exciting new approaches to the problem. This paper describes preliminary work on a coupled oscillator control scheme for a four-legged robot. The eventual goal is to use both distributed and hierarchical controllers which roughly correspond to models for the animal locomotory control system proposed in the neural science literature. As a first step, the effect of a simple local feedback at each of four springy legs on a platform is examined. Using the method of averaging, it is found that stable oscillations occur which correspond to four-legged animal gaits. In addition, numerical experiments are used to demonstrate the feasibility of performing gait transitions using a coupled oscillator controller.

1 Introduction

Research on artificial legged locomotion has the potential for producing vehicles and mobile robots which are capable of easily crossing rocky terrain, climbing or jumping over large obstacles, and agilely maneuvering in tight surroundings. Specific examples of needs for these capabilities include Mars exploration, military assault or transport, underwater exploration, and hazardous site inspection. A further benefit to research in this area is the insight it gives into the animal locomotory control system.

Progress over the years has been both significant and slow. Raibert (1986) and Song & Waldron (1989) contain nice descriptions of the history. One stumbling block to achieving effective legged robot control is the fact that the problem does not seem to fit well into the framework of modern nonlinear control theory. For example, the equations of motion for a legged animal or robot are a function of exactly which legs are on the ground. During one cycle of a gait, then, very different dynamics apply at different stages of the cycle. If one attempts to treat each of these stages separately, then it is difficult to ensure that transitions between the stages are smooth and natural. Another difficulty is in defining an appropriate output for the legged system. For many cases, all that is really important is that the robot or vehicle move from point A to point B. How does one map the simple A to B description into joint angle trajectories (which typically must satisfy many constraints) and thus control inputs? Finally, the fact that a legged animal or robot usually has many degrees of freedom further complicates all of this. Perhaps due to the above difficulties, a review of work on artificial legged locomotion leaves one with the impression that straightforward application of nonlinear control theory to the problem has produced somewhat limited success, whereas innovative control approaches which depart from the standard methods have usually been involved in the "breakthroughs."

An area of research that has recently excited many doing work in legged robot control is the modeling of animal central pattern generators by networks of coupled oscillators. Central pattern generators are a part of the nervous system which generate signals to stimulate many of the periodic motions in an animal such as chewing, scratching, and running. It is possible that through investigation of coupled oscillators, effective control algorithms for legged robots may be developed. In addition, this approach should provide additional insight into the animal locomotory control system since it is biologically inspired.

At the Robotics Laboratory at Boston University, work is beginning on a four-legged robot which will be able to run with a variety of gaits. It will be controlled by a network of coupled oscillators, and the overall control scheme will be both distributed and hierarchical (as also is the case in nature). The initial, modest goal is to obtain "running-in-place" motions. This simply means that the robot will stably use the correct sequence of foot placements for several gaits without moving forward. It is hoped that forward motion can be added on later without too much difficulty.

The paper continues as follows: Section 2 reviews some of the relevant previous work in applied coupled oscillator theory and robotics. In Section 3 the main results are presented: Using the method of averaging, the dynamics of a platform with four springy legs and simple local feedback are shown to contain stable periodic oscillations corresponding to gaits for four-legged animals. Furthermore, the ability to make transitions between different gaits is also addressed. Future work is discussed in Section 4 and conclusions are offered in

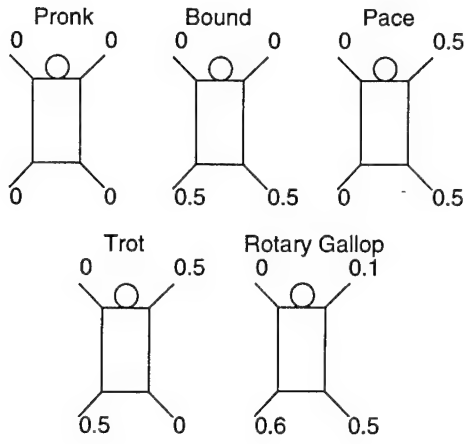

Figure 1: Phase Relationships for Different Gaits (adapted from Alexander (1984)). The numbers are fractions of one period and indicate when the corresponding leg strikes the ground relative to the left-front leg.

Section 5.

2 Background

2.1 Four-Legged Animal Gaits

A description of four-legged animal gaits can be found in, for example, Alexander (1984) and Hildebrand (1989). In addition to discussing animal gaits, Alexander (1984) points out that animal tendons are capable of storing and releasing energy in much the same manner as a spring. The robot discussed here will also have elastic storage of energy. Distinctions between gaits are often somewhat arbitrary (Hildebrand 1989), but, for the purposes of this discussion, the phase relationships shown in Figure 1 will be assumed. It should be noted that, although animals usually use several gaits, there is probably not a single animals which uses all of the gaits in Figure 1. Specific examples of animals using these gaits are *pronk:* deer, *bound:* house mouse, *pace:* camel, *trot:* horse, *rotary gallop:* cheetah (Hildebrand 1989).

2.2 The Animal Locomotory Control System

Somewhat surprisingly, researchers have found that there are fundamental similarities between the locomotory control system for animals as diverse as the cockroach and the cat (Pearson 1976). The animal motor control system responsible for locomotion is frequently discussed in terms of four components: command systems, coordinating systems, limb central pattern generators, and sensory feedback mechanisms. Ayers & Crisman (1993) refer to this as the CCCPG model. The four-legged robot project currently underway at Boston University will eventually incorporate simple versions of each of these systems. However, this paper focuses mainly on the effects of a simple scheme to incorporate sensory feedback.

It is now well-known that the generation of rhythmic locomotory patterns by the nervous system does not depend on sensory input, but when present, this feedback modulates muscle motions to better control the gait. For example, preventing a cat's leg from fully extending during a stance phase will also prevent the initiation of the swing phase (Gordon 1991). Feedback is especially important when the environment imposes unexpected perturbations on the animal. For example, the animal might step in a small hole, the surface might become slippery or soft, or the animal might be forced to pull a cart. Pearson & Duysens (1976) describes experiments on both cockroaches and cats which indicate that both position and load sensing of muscles are used to help control locomotion.

The animal locomotory control system is organized in both a distributed and hierarchical fashion. During locomotion, localized control systems help to maintain the proper gait motions in response to sensed position and force. Inspired by this idea, the simple model described in this paper has four local controllers, each of which applies energy damping and pumping. Without any coupling between the legs, the local controllers would produce uncoordinated leg oscillations. However, when the legs are coupled through the body, particular patterns of oscillation occur. These correspond roughly to some observed gaits for four-legged animals.

2.3 Coupled Oscillators for Modeling CPGs

An nice introduction to coupled oscillators can be found in in Strogatz & Stewart (1993). This particular branch of mathematics was initiated by the Dutch physicist Christiaan Huygens who noticed that the pendulums of two clocks became synchronized when hung near one another on a wall. This was due to the very weak coupling of their motions provided by the wall. Coupled oscillators have been used to model central pattern generators in animals.

The basic periodic motion of an animal's limbs involved in locomotion is thought to be produced by central pattern generators. Central pattern generators are believed to be made up of closed circuits of inter-neurons that re-excite themselves (Gordon 1991). The central pattern generators which are responsible for locomotion are located in intrinsic spinal circuits. This has been demonstrated by severing connections with the higher level functions. Each limb of an animal has its own central pattern generator; experiments have demonstrated that animals will continue to cycle a leg that is on a treadmill even if the other leg is still. Of course, in normal walking or running the oscillations are coupled and a constant phase relationship is maintained. However, the phase depends on the particular gait, and it is therefore crucial that independent oscillators control the legs. Since spinal circuits take care of much of the details of muscle coordination for locomotion, the higher level control systems need only specify general commands such as the amplitude of the motion (Gordon 1991).

Note that in this paper, the coupled oscillations that are discussed occur in a particular physical system which is an initial attempt at a dynamic model of a four-legged animal or robot with sensory feedback. Eventually, a coupled oscillator controller is planned which will be based on the work described in this subsection.

Rand, Cohen & Holmes (1988) contains a nice description of the mathematical analysis of coupled oscillators and their relationship to the behavior of central pattern generators. The

individual oscillators are particularly simple, each having only one state variable. The work of Kopell (1988) involves more complicated oscillators which seem to be more closely tied to biology. Kopell specifically considered the role of central pattern generators in producing the undulatory motion used by swimming fish. Collins & Stewart (1993) looked at the oscillation patterns expected of networks with symmetrically arranged oscillator types and couplings. The patterns they obtained agreed very well with observed gaits of four-legged animals. Gaits obtained in simulations of four coupled oscillators included the pronk, trot, gallop, pace, and bound. The lack of any specific model for the oscillators and their couplings makes the analysis quite general and of use to roboticists looking for an appropriate structure for coupled oscillator control. Indeed, their paper was a source of inspiration for initiating this research project. Collins & Richmond (1994) added command inputs to their previous work to generate gait transitions for their network of four coupled oscillators. The command inputs changed the network's driving signal and/or altered internal parameters of the limb CPG oscillators. This caused the network to perform walk-to-trot, walk-to-bound, trot-to-walk, and trot-to-bound transitions. None of the mathematical analysis has yet considered the use of sensory feedback or the interaction of the coupled oscillators with animal musculoskeletal dynamics. This paper is a preliminary attempt to include such important effects.

2.4 Raibert's Four-Legged Robot

Raibert (1986) and Raibert (1990) give details on this famous four-legged robot. Trotting, pacing, and bounding were all achieved in a physical system. By considering the legs which moved together (e.g., diagonal legs for a trot) as one *virtual leg*, Raibert was able to use control algorithms for his biped robot which were, in turn, based on control algorithms for his one-legged robot. Raibert divided control into three parts: control of hopping height, control of forward running speed, and control of attitude. The control of all three was done independently. This paper is primarily concerned with hopping height and attitude. Running speed will be considered at a later time. In contrast to Raibert's approach, the method proposed here will not build directly upon one-legged hopping results. Instead, the dynamics of a four-legged platform will be considered independently. One motivating factor for this departure is the intuitive belief that stabilizing a four-legged robot should be inherently easier than a one-legged robot. Strangely, besides the work by Raibert, little has been done on the control of dynamically-stable four-legged robots.

2.5 Coupled Oscillator Control of Legged Robots

Chiel, Beer, Quinn & Espenschied (1992) describe experiments demonstrating the robustness of a simple six-legged robot. The locomotion controller was an artificial neural network modeled after the cockroach nervous system. This work was an implementation of the ideas of Chiel, Beer & Sterling (1989). Ayers & Crisman (1993) used an artificial neural network based on a slightly more abstract model of the animal motor control system. Their ultimate goal was to construct an eight-legged robot capable of walking in turbulent shallow water. Lewis, Fagg & Solidum (1992) also used an artificial neural network to control a six-legged robot. Genetic algorithms automatically adjusted the weights and thresholds on the neurons until satisfactory locomotion was achieved. Bay & Hemami (1987) showed that

four coupled van der Pol oscillators could produce joint angle trajectories for walking and jumping in a four-link biped model. The dynamics of the biped were not considered in their simulations, however. Katoh & Mori (1984) used two coupled van der Pol oscillators to generate joint angle trajectories for a planar biped robot. Their controller was based on the linearized equations of motion, but simulations were performed on the full nonlinear model. The motion of the robot was stable since the robot's trajectory was made to be that of the van der Pol oscillator. Marvin (1992) used a network of six coupled oscillators to generate gaits for a Walking Stick Insect model. Simulations included the full dynamics of the insect, although only statically-stable gaits were tested. Performance was best for the slower gaits. Mishra (1993) used coupled oscillators to control a simulation of a planar biped robot. Pulse coupling was used to provide interaction between the oscillators and the mechanical system while continuous coupling was used for interaction between the oscillators of the controller. This control philosophy is the most similar to what is discussed here.

At this point it is important to point out that few of the coupled oscillator projects (even fewer of those with experiments) have involved gaits in which there were dynamic motions of the legged robot. Full (1993) stresses the importance of considering dynamic effects in understanding animal locomotion control.

The previous review of the literature suggests that, although much progress has been made in modeling the animal CPG using coupled oscillator theory, further work remains in understanding the coupling of the CPG to the animal musculoskeletal dynamics, and in applying this to dynamic legged robot control. The main results of this paper are presented in the next section. These results suggest that for dynamic gaits, it may be possible to view musculoskeletal dynamics as consisting of coupled oscillations producing various types of gaits. These dynamics can be, in turn, coupled to the CPG dynamics for additional stability and control.

3 Platform Dynamics

The four-legged platform dynamics are best understood by considering one and two degree-of-freedom systems first.

3.1 One Degree of Freedom

3.1.1 Equations of Motion

Consider the simple system in Figure 2. The damper is present to model dissipative forces in the spring, actuator, and sensors. An ideal actuator is assumed, which can apply a force f' between the mass and ground. Also assumed (but not pictured) are sensors which are capable of measuring both the position and velocity (i.e., the state) of the mass. The equation of motion is

$$\ddot{z} + \frac{b'}{m}\dot{z} + \frac{k}{m}z = \frac{1}{m}f' \tag{1}$$

This system can be thought of as a very crude model of an animal leg with the spring representing tendon stiffness. Similarly the system could represent one of the four legs of a quadruped robot. The current model has the leg fixed to the ground, but this restriction

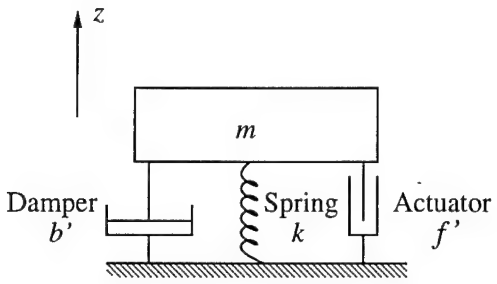

Figure 2: One Degree-of-Freedom Mechanism and Associated Variables. Not shown are sensors for measuring z and $\dot{z}$.

will be lifted in future work. It is expected that, at least qualitatively, similar results will be obtained: If the foot were allowed to leave the ground, gravity would become the restoring force instead of the spring.

The goal here is to introduce a feedback which will produce a periodic variation in the mass position z. This feedback might correspond to a reflex in a legged animal. Furthermore, it is desired that this be accomplished in a relatively "efficient" manner, e.g., using small force, f'. A logical approach is simply to excite the natural resonance of the system. Although there are many feedbacks which would satisfy these goals, the following was chosen for this study:

$$f' = (a - bz^2)\dot{z} \tag{2}$$

where a and b are positive gains which can be set by the operator. Negative damping (energy pumping) is applied for $-\sqrt{a/b} < z < \sqrt{a/b}$ and positive damping (energy dissipation) is applied for z outside this range. Thus, it is not surprising that, for suitable values of a and b, a limit cycle is created involving a periodic oscillation of z as desired. Note that a simple sinusoidal function of time at the correct frequency would also produce a periodic variation of z as a function of time, but feedback has the advantage of better handling perturbations imposed by the external environment. Suppose, for example, that an additional mass, m', was set on top of the mass m in Figure 2. This would change the resonant frequency, and a forcing function which worked for the single mass m would not work for the combination $m + m'$ for m' sufficiently large. On the other hand, the feedback (2) would continue to produce periodic variations of z, although the frequency of oscillation would change. Substituting equation (2) into equation (1) results in

$$\ddot{z} + \frac{1}{m}(bz^2 - (a - b'))\dot{z} + \frac{k}{m}z = 0$$

To put this equation in a simpler and more familiar form, let $\epsilon = (a - b')/m > 0$, $\epsilon c = b/m$, and $\omega_0^2 = k/m$. This results in

$$\ddot{z} + \epsilon(cz^2 - 1)\dot{z} + \omega_0^2 z = 0$$

However, c and ω_0 are not critical parameters since they can be eliminated by scaling z and time, respectively. So, it will be more convenient to use instead

$$\ddot{z} + \epsilon(z^2 - 1)\dot{z} + z = 0 \tag{3}$$

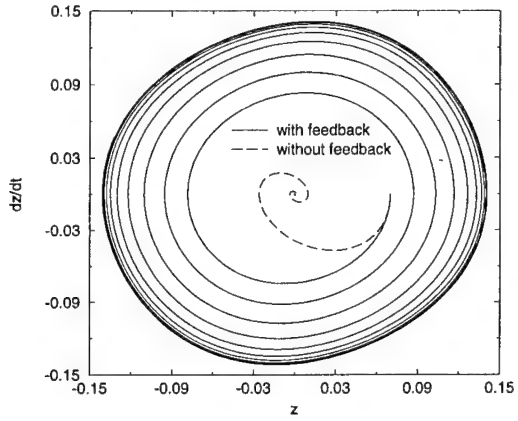

Figure 3: Comparison of phase space trajectories for simulations. "with feedback" corresponds to the equation $\ddot{z} + 0.1(200z^2 - 1)\dot{z} + z = 0$ and "without feedback" corresponds to $\ddot{z} + 0.6\dot{z} + z = 0$.

where it is understood that z and time may be arbitrarily scaled. This is an example of the famous van der Pol oscillator equation (Guckenheimer & Holmes 1983). It is well-known that for $\epsilon > 0$, small, this equation has an unstable equilibrium, $(z, \dot{z}) = (0, 0)$, and a stable limit cycle of approximate frequency 1 and approximate magnitude 2. Figure 3 shows phase space plots of a numerical simulation of equation (1) with $b'/m = 0.6$, $k/m = 1$, and $f' = 0$ and equation (3) where z has been scaled by a factor of $1/\sqrt{50}$.

Next, the method of averaging will be applied to equation (3) in order to determine the magnitude, frequency, and stability of the closed orbit. This information is already known, but averaging will also be used for the more complicated two and three degree-of-freedom systems which will build on the one degree-of-freedom result.

3.1.2 The Averaged Equation

Guckenheimer & Holmes (1983) give a nice description of the Averaging Theorem although the slightly more general version of Hale (1980) will be needed for this paper. Briefly, given a system

$$\dot{x} = \epsilon f(x, t), \; x \in \mathbb{R}^n \tag{4}$$

where f is almost periodic in t[1] and $\epsilon > 0$, small, one studies instead the "averaged" equation

$$\dot{x} = \epsilon f_0(x) \tag{5}$$

where

$$f_0(x) = \lim_{T \to \infty} \frac{1}{T} \int_0^T f(x, t) dt \tag{6}$$

Under additional technical conditions (Hale 1980),

[1]The set of almost periodic functions includes, for example, all periodic functions and sums of periodic functions (e.g., $\sin t + \sin \sqrt{3}t$ is not periodic but is almost periodic.) For details see Hale (1980).

1. If the averaged equation (5) contains a hyperbolic fixed point, x_0, then the original equation (4) contains an almost periodic hyperbolic orbit $\gamma(t) \approx x_0$ of the same stability type as x_0.

2. If the original system has f periodic in t, then if the averaged equation (5) contains a hyperbolic fixed point, x_0, then the original equation (4) contains a periodic hyperbolic orbit $\gamma(t) \approx x_0$ of the same stability type as x_0.

Equation (3) can be put into the form of equation (4) through application of the van der Pol transformation (Guckenheimer & Holmes 1983) which has the effect of "slowing down" the oscillations. Let $z = x_1$, $\dot{z} = x_2$ and

$$\begin{bmatrix} u_1 \\ u_2 \end{bmatrix} = \begin{bmatrix} \cos t & -\sin t \\ -\sin t & -\cos t \end{bmatrix} \begin{bmatrix} x_1 \\ x_2 \end{bmatrix} \tag{7}$$

Applying this to equation (3) one obtains

$$\begin{aligned} \dot{u}_1 &= \epsilon \sin t((u_1 \cos t - u_2 \sin t)^2 - 1)(-u_1 \sin t - u_2 \cos t) \\ \dot{u}_2 &= \epsilon \cos t((u_1 \cos t - u_2 \sin t)^2 - 1)(-u_1 \sin t - u_2 \cos t) \end{aligned}$$

which is in the correct form to apply the averaging method. Integrating as in equation (6) yields

$$\begin{aligned} \dot{u}_1 &= \frac{\epsilon}{2} u_1 \left(1 - \frac{u_1^2 + u_2^2}{4}\right) \\ \dot{u}_2 &= \frac{\epsilon}{2} u_2 \left(1 - \frac{u_1^2 + u_2^2}{4}\right) \end{aligned}$$

Finally, converting to polar coordinates gives

$$\begin{aligned} \dot{r} &= \frac{\epsilon}{2} r \left(1 - \frac{r^2}{4}\right) \\ \dot{\theta} &= 0 \end{aligned}$$

Linearizing the r vector field shows that this set of equations has an unstable fixed point at $r = 0$ and an attracting circle of fixed points at $r = 2$. The $r = 2$ equilibria corresponds to a solution $z(t) \approx 2\cos(t + \psi_0)$, where ψ_0 is arbitrary, for the original system (3).

3.2 Two Degrees of Freedom

3.2.1 Equations of Motion

Figure 4 shows the system to be considered in this section. For small values of θ, the height of the left and right sides are approximately given by $z_l = z - w\theta/2$ and $z_r = z + w\theta/2$, respectively. Now, assume a uniformly distributed mass in the horizontal direction, and a negligible platform height in the vertical direction. The inertia about the center of mass is then $mw^2/12$. Also, assume identical springs and dampers on each side of the platform

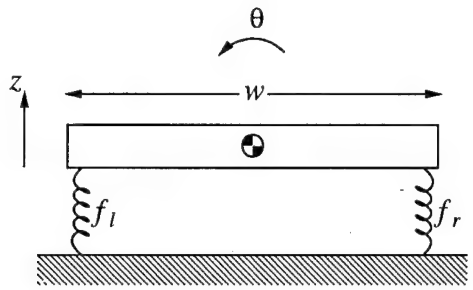

Figure 4: Two Degree-of-Freedom Mechanism. For simplicity, sensors, actuators, and dampers are not shown. f_l and f_r represent the total forces on the left and right sides, respectively.

and actuator forces f_l' and f_r' on the left and right sides, respectively. Then, for small oscillations, the equations of motion are

$$\ddot{z} + \frac{2b'}{m}\dot{z} + \frac{2k}{m}z = \frac{1}{m}(f_l' + f_r') \tag{8}$$

$$\ddot{\theta} + \frac{6b'}{m}\dot{\theta} + \frac{6k}{m}\theta = \frac{6}{mw}(-f_l' + f_r') \tag{9}$$

Note that if the actuator forces are zero, the dynamics of z and θ are independent. This result depends on the assumption of identical springs and dampers; if there were slight differences in spring constants, for example, there would be coupling between the two equations. The two cases of interest will be oscillations of z with $\theta \equiv 0$ and oscillations of θ with $z \equiv 0$. In the first case the left and right sides oscillate in phase, while in the second case the left and right sides oscillate out of phase. Finally, also notice that under the assumptions of a uniformly distributed mass, the natural resonance frequency for θ is $\sqrt{3}$ times the resonance frequency for z. An interesting topic for future work will be allowing the inertia to be a free parameter and then examining the bifurcations as the inertia varies.

Analogously to Section 3.1.1 the following feedback is chosen for the left and right sides:

$$f_l' = (a - bz_l^2)\dot{z}_l \tag{10}$$

$$f_r' = (a - bz_r^2)\dot{z}_r \tag{11}$$

This can be considered "local feedback" since the feedback for the left side depends only on the state of the left side, and the feedback for the right side depends only on the state of the right side.

Now, substituting equations (10) and (11) into (8) results in

$$\ddot{z} + \frac{2}{m}(bz^2 - (a - b'))\dot{z} + \frac{2k}{m}z = -\frac{bw^2}{2m}\theta(\theta\dot{z} + 2\dot{\theta}z)$$

Similarly, substituting equations (10) and (11) into (9) results in

$$\ddot{\theta} + \frac{6}{m}\left(b\frac{w^2}{4}\theta^2 - (a - b')\right)\dot{\theta} + \frac{6k}{m}\theta = -\frac{6b}{m}z(\dot{\theta}z + 2\theta\dot{z})$$

Choosing the new parameters $\epsilon = 2(a-b')/m$, $\epsilon c = 2b/m$, and $\omega_0^2 = 2k/m$ gives

$$\begin{aligned} \ddot{z} + \epsilon(cz^2 - 1)\dot{z} + \omega_0^2 z &= -\epsilon c\frac{w^2}{4}\theta(\theta\dot{z} + 2\dot{\theta}z) \\ \ddot{\theta} + 3\epsilon\left(c\frac{w^2}{4}\theta^2 - 1\right)\dot{\theta} + 3\omega_0^2\theta &= -3\epsilon cz(\dot{\theta}z + 2\theta\dot{z}) \end{aligned}$$

c, w, and ω_0 are not critical parameters since they can be eliminated by scaling z, θ, and time. So, without loss of generality, the following equations will be used:

$$\ddot{z} + \epsilon(z^2 - 1)\dot{z} + z = -\epsilon\theta(\theta\dot{z} + 2\dot{\theta}z) \quad (12)$$

$$\ddot{\theta} + 3\epsilon\left(\theta^2 - 1\right)\dot{\theta} + 3\theta = -3\epsilon z(\dot{\theta}z + 2\theta\dot{z}) \quad (13)$$

Notice that the system of equations (12) and (13) describe coupled van der Pol oscillators. The left-hand-sides of the equations are the oscillator equations, and the right-hand-sides are the coupling terms.

3.2.2 The Averaged Equations

Equations (12) and (13) can be put into the appropriate form for averaging by applying the transformation (7), letting $y_1 = \theta$ and $y_2 = \dot{\theta}$, and applying another van der Pol transformation:

$$\begin{bmatrix} v_1 \\ v_2 \end{bmatrix} = \begin{bmatrix} \cos\sqrt{3}t & -\frac{1}{\sqrt{3}}\sin\sqrt{3}t \\ -\sin\sqrt{3}t & -\frac{1}{\sqrt{3}}\cos\sqrt{3}t \end{bmatrix} \begin{bmatrix} y_1 \\ y_2 \end{bmatrix} \quad (14)$$

Note that in this case, the resulting vector field is not periodic but is almost periodic. Following the same procedure as in Section 3.1.2 yields the averaged equations

$$\begin{aligned} \dot{u}_1 &= \frac{\epsilon}{2}u_1\left(1 - \frac{u_1^2 + u_2^2}{4}\right) - \frac{\epsilon}{4}u_1(v_1^2 + v_2^2) \\ \dot{u}_2 &= \frac{\epsilon}{2}u_2\left(1 - \frac{u_1^2 + u_2^2}{4}\right) - \frac{\epsilon}{4}u_2(v_1^2 + v_2^2) \\ \dot{v}_1 &= \frac{3\epsilon}{2}v_1\left(1 - \frac{v_1^2 + v_2^2}{4}\right) - \frac{3\epsilon}{4}v_1(u_1^2 + u_2^2) \\ \dot{v}_2 &= \frac{3\epsilon}{2}v_2\left(1 - \frac{v_1^2 + v_2^2}{4}\right) - \frac{3\epsilon}{4}v_2(u_1^2 + u_2^2) \end{aligned}$$

Converting to polar coordinates, r_u being associated with u_1 and u_2 and r_v being associated with v_1 and v_2, gives

$$\dot{r}_u = \frac{\epsilon}{2}r_u\left(1 - \frac{r_u^2}{4}\right) - \frac{\epsilon}{4}r_u r_v^2 \quad (15)$$

$$\dot{\theta}_u = 0 \quad (16)$$

$$\dot{r}_v = \frac{3\epsilon}{2}r_v\left(1 - \frac{r_v^2}{4}\right) - \frac{3\epsilon}{4}r_v r_u^2 \quad (17)$$

$$\dot{\theta}_v = 0 \quad (18)$$

There are a total of four equilibria to the system of equations (15), (17):

1. $r_u = r_v = 0$; *unstable:* This corresponds to $z(t) = \theta(t) = 0$ for the original system of equations (12) and (13).

2. $r_u = 2/\sqrt{3}$, $r_v = 2/\sqrt{3}$; *unstable:* This corresponds to

$$\begin{aligned} z(t) &\approx (2/\sqrt{3})(\cos t + \psi_{z0}) \\ \theta(t) &\approx (2/\sqrt{3})\cos(\sqrt{3}t + \psi_{\theta 0}) \end{aligned}$$

   where ψ_{z0} and $\psi_{\theta 0}$ are arbitrary.

3. $r_u = 2$, $r_v = 0$; *stable:* This corresponds to

$$\begin{aligned} z(t) &\approx 2\cos(t + \psi_{z0}) \\ \theta(t) &= 0 \end{aligned}$$

4. $r_u = 0$, and $r_v = 2$; *stable:* This corresponds to

$$\begin{aligned} z(t) &= 0 \\ \theta(t) &\approx 2\cos(\sqrt{3}t + \psi_{\theta 0}) \end{aligned}$$

Cases 3 and 4 are the most important since only stable solutions can typically be observed in any physical system. Case 3 involves in-phase oscillations of the left and right sides of the platform in Figure 4 and is the planar version of the pronk phase relationship. Case 4 involves oscillations where the left and right sides of the platform are 180° out of phase and could be considered the planar version of the bound or pace.

Results of simulations of equations (12) and (13) are shown in Figure 5. Figure 6 shows a phase portrait for equations (15) and (17). Notice that regions of attraction are reasonably large for both stable solutions.

The situation is relatively straightforward here due to incommensurate resonant frequencies for z and θ. As shall be seen in Section 3.3, when oscillators with identical frequencies are coupled, there are equilibria sets instead of simple isolated equilibria in the averaged equations.

3.3 Three Degrees of Freedom

3.3.1 Equations of Motion

Finally, consider the system in Figure 7. Understanding this system was the major goal of this study. For small values of θ and ϕ, the equations of motion may be approximated as

$$\begin{aligned} m\ddot{z} &= f_{lf} + f_{rf} + f_{lb} + f_{rb} \\ I_{yy}\ddot{\theta} &= \frac{w}{2}(-f_{lf} + f_{rf} - f_{lb} + f_{rb}) \\ I_{xx}\ddot{\phi} &= \frac{l}{2}(-f_{lf} - f_{rf} + f_{lb} + f_{rb}) \end{aligned}$$

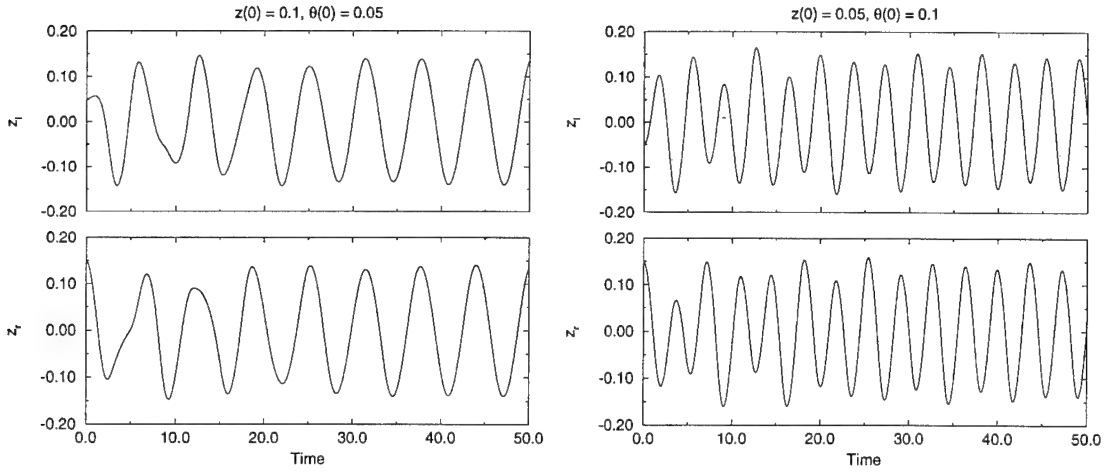

Figure 5: *Left:* Stable In-Phase Oscillations of Left and Right Sides (Case 3). *Right:* Stable Out-of-Phase Oscillations of Left and Right Sides (Case 4). Both plots are results of simulations of equations (12) and (13) with $\epsilon = 0.1$ and z and θ scaled by $1/\sqrt{50}$. The left and right heights are given by $z_l = z - w\theta/2$ and $z_r = z + w\theta/2$.

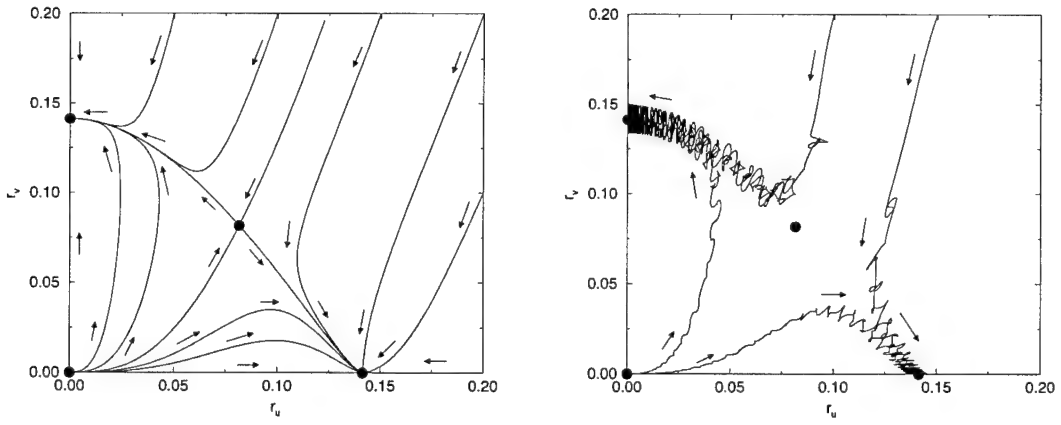

Figure 6: *Left:* Phase Portrait of Oscillation Magnitudes Using Averaged Equations. Results were obtained by simulating equations (15) and (17) with $\epsilon = 0.1$ and z and θ scaled by $1/\sqrt{50}$. *Right:* A Few Oscillation Magnitude Trajectories Before Averaging. Equations (12) and (13) were simulated with $\epsilon = 0.1$, and z and θ scaled by $1/\sqrt{50}$. Solid circles indicate equilibria locations.

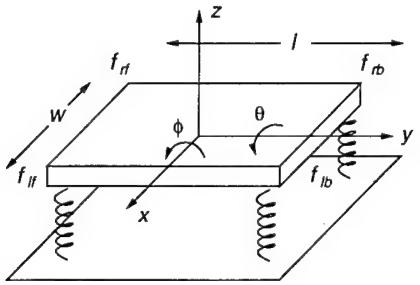

Figure 7: Three Degree-of-Freedom Mechanism.

where subscripts l and r denote left and right, and f and b denote front and back. The reader may be concerned about the many terms in the equations of motion that are neglected here, however, simulations of the full dynamics with the feedback described below have verified that, for small oscillations, the terms above are indeed dominant, and nothing important is lost. Again, identical springs and dampers are assumed at each corner, and the platform mass is assumed to be uniformly distributed in the horizontal plane and negligible in the vertical direction. The feedback at each corner is

$$f_i' = (a - bz_i^2)\dot{z}_i, \; i \in \{lf, rf, lb, rb\} \tag{19}$$

where $z_{lf} = z - w\theta/2 - l\phi/2$ is the height of the left-front corner, and the remaining heights are defined similarly. After all substitutions are made, one finds that the resonant frequencies for θ and ϕ are identical and are $\sqrt{3}$ times the resonant frequency for z. This is true regardless of the values for the parameters w and l. Varying these lengths changes the inertia about the corresponding axis, but, at the same time, it also scales the torque applied about the same axis. The two effects cancel, and the frequency stays the same.

Now, the resulting equations involve a number of parameters which are non-essential including w and l which simply scale the variables. Eliminating these parameters gives the following coupled oscillator equations:

$$\ddot{z} + \epsilon(z^2 - 1)\dot{z} + z = -\epsilon\dot{z}(\theta^2 + \phi^2) - 2\epsilon z(\theta\dot{\theta} + \phi\dot{\phi}) \tag{20}$$

$$\ddot{\theta} + 3\epsilon(\theta^2 - 1)\dot{\theta} + 3\theta = -3\epsilon\dot{\theta}(z^2 + \phi^2) - 6\epsilon\theta(z\dot{z} + \phi\dot{\phi}) \tag{21}$$

$$\ddot{\phi} + 3\epsilon(\phi^2 - 1)\dot{\phi} + 3\phi = -3\epsilon\dot{\phi}(z^2 + \theta^2) - 6\epsilon\phi(z\dot{z} + \theta\dot{\theta}) \tag{22}$$

It is easy to verify that setting $\phi \equiv 0$ in equations (20), (21) yields the equations (12), (13) for the two degree-of-freedom system. Note that two of the oscillators have identical resonant frequencies which are incommensurate with the third.

3.3.2 The Averaged Equations

Proceeding in a manner analogous to Section 3.2.2 one obtains the averaged equations.

$$\dot{u}_1 = \frac{\epsilon}{2}u_1\left(1 - \frac{u_1^2 + u_2^2}{4}\right) - \frac{\epsilon}{4}u_1(v_1^2 + v_2^2 + w_1^2 + w_2^2)$$

$$\dot{u}_2 = \frac{\epsilon}{2}u_2\left(1 - \frac{u_1^2 + u_2^2}{4}\right) - \frac{\epsilon}{4}u_2(v_1^2 + v_2^2 + w_1^2 + w_2^2)$$

$$\begin{aligned}
\dot{v}_1 &= \frac{3\epsilon}{2}v_1\left(1-\frac{v_1^2+v_2^2}{4}\right)-\frac{3\epsilon}{4}v_1(u_1^2+u_2^2)-\frac{3\epsilon}{8}v_1(w_1^2+w_2^2)-\frac{3\epsilon}{4}w_1(v_1w_1+v_2w_2)\\
\dot{v}_2 &= \frac{3\epsilon}{2}v_2\left(1-\frac{v_1^2+v_2^2}{4}\right)-\frac{3\epsilon}{4}v_2(u_1^2+u_2^2)-\frac{3\epsilon}{8}v_2(w_1^2+w_2^2)-\frac{3\epsilon}{4}w_2(v_1w_1+v_2w_2)\\
\dot{w}_1 &= \frac{3\epsilon}{2}w_1\left(1-\frac{w_1^2+w_2^2}{4}\right)-\frac{3\epsilon}{4}w_1(u_1^2+u_2^2)-\frac{3\epsilon}{8}w_1(v_1^2+v_2^2)-\frac{3\epsilon}{4}v_1(v_1w_1+v_2w_2)\\
\dot{w}_2 &= \frac{3\epsilon}{2}w_2\left(1-\frac{w_1^2+w_2^2}{4}\right)-\frac{3\epsilon}{4}w_2(u_1^2+u_2^2)-\frac{3\epsilon}{8}w_2(v_1^2+v_2^2)-\frac{3\epsilon}{4}v_2(v_1w_1+v_2w_2)
\end{aligned}$$

Converting to polar coordinates (r_u associated with u_1 and u_2, etc.) yields

$$\dot{r}_u = \frac{\epsilon}{2}r_u\left(1-\frac{r_u^2}{4}\right)-\frac{\epsilon}{4}r_u(r_v^2+r_w^2) \tag{23}$$

$$\dot{\theta}_u = 0 \tag{24}$$

$$\dot{r}_v = \frac{3\epsilon}{2}r_v\left(1-\frac{r_v^2}{4}\right)-\frac{3\epsilon}{4}r_vr_u^2-\frac{3\epsilon}{8}r_vr_w^2-\frac{3\epsilon}{4}r_vr_w^2\cos^2(\theta_w-\theta_v) \tag{25}$$

$$\dot{\theta}_v = -\frac{3\epsilon}{8}r_w^2\sin[2(\theta_w-\theta_v)] \tag{26}$$

$$\dot{r}_w = \frac{3\epsilon}{2}r_w\left(1-\frac{r_w^2}{4}\right)-\frac{3\epsilon}{4}r_wr_u^2-\frac{3\epsilon}{8}r_wr_v^2-\frac{3\epsilon}{4}r_v^2r_w\cos^2(\theta_v-\theta_w) \tag{27}$$

$$\dot{\theta}_w = -\frac{3\epsilon}{8}r_v^2\sin[2(\theta_v-\theta_w)] \tag{28}$$

In the three degree-of-freedom case, the phenomenon of *phase locking* is observed as evidenced by equations (26) and (28). Note that equations (26) and (28) are irrelevant if either r_v or r_w is 0.

The set of equations (23), (25) – (28) has the following equilibria:

1. $r_u = r_v = r_w = 0$; *unstable:* This corresponds to $z(t) = \theta(t) = \phi(t) = 0$ for the original set of equations (20) – (22).

2. $r_u = 0$, $r_v = r_w = 1$, $\theta_w - \theta_v = 0,\ \pi$; *unstable:* This corresponds to

$$\begin{aligned}
z(t) &= 0\\
\theta(t) &\approx \cos(\sqrt{3}t+\psi_0)\\
\phi(t) &\approx \pm\cos(\sqrt{3}t+\psi_0)
\end{aligned}$$

3. $r_u = 2/\sqrt{3}$, $\{(r_v, r_w) : r_v, r_w \geq 0,\ r_v^2+r_w^2 = 4/3\}$, $\theta_v - \theta_w = \pi/2,\ 3\pi/2$; *unstable:* This corresponds to

$$\begin{aligned}
z(t) &\approx (2/\sqrt{3})\cos(t+\psi_{z0})\\
\theta(t) &\approx \alpha\cos(\sqrt{3}t+\psi_0)\\
\phi(t) &\approx \pm\sqrt{4/3-\alpha^2}\sin(\sqrt{3}t+\psi_0)
\end{aligned}$$

where the free parameter α satisfies $\alpha \in [0, 2/\sqrt{3}] \subset \mathbb{R}$.

4. $r_u = 2$, $r_v = r_w = 0$; *stable:* This corresponds to

$$\begin{aligned} z(t) &\approx 2\cos(t + \psi_{z0}) \\ \theta(t) &= 0 \\ \phi(t) &= 0 \end{aligned}$$

5. $r_u = 0$, $\{(r_v, r_w) : r_v, r_w \geq 0,\ r_v^2 + r_w^2 = 4\}$, $\theta_w - \theta_v = \pi/2,\ 3\pi/2$; *stable:* This corresponds to

$$\begin{aligned} z(t) &= 0 \\ \theta(t) &\approx \alpha\cos(\sqrt{3}t + \psi_0) \\ \phi(t) &\approx \pm\sqrt{4 - \alpha^2}\sin(\sqrt{3}t + \psi_0) \end{aligned}$$

where the free parameter α satisfies $\alpha \in [0, 2] \subset \mathbb{R}$.

Recall that for the two degree-of-freedom case, the stable solutions corresponded to oscillations of variables associated with one oscillator while the other variables were identically zero. Evidently, this was because the two resonant frequencies were incommensurate. Now, for the three degree-of-freedom case, coupled oscillators with identical frequencies occur, and instead of isolated closed orbits, solutions with a continuum of orbits exist. Note that a slight perturbation of the resonant frequency for one of the identical oscillators would dramatically change the nature of the periodic solutions (bifurcation). With three incommensurate frequencies present, one would expect three stable solutions each associated with oscillations of variables of only one of the oscillators.

Case 4 corresponds to the pronk gait of a four legged animal since all four corners of the platform in Figure 7 would move up and down synchronously. Figure 8 (top) shows convergence to this solution. Case 5 contains the bound, rotary gallop, and pace-type motions. For the bound, let $\alpha = 0$ to produce front-to-back oscillations. This is displayed in Figure 8 (bottom). For the pace, let $\alpha = 2$ to produce left-to-right oscillations. Figure 9 (top) shows an example of this. Finally, the rotary gallop corresponds to $0 < \alpha < 2$. Since oscillations of θ and ϕ are 90° out of phase, the four corners oscillate vertically in a rotary pattern as in Figure 9 (bottom).

3.4 Gait Transitions

Having described the dynamics of the platform with simple, local feedback, the problem of higher-level control will now be briefly considered. The platform can perform the pronk, bound, rotary gallop, and pace, but there are a few problems. First of all, the bound, rotary gallop, and pace are not asymptotically stable motions; any slight perturbation will cause a shift in the oscillation patterns. Secondly, a mechanism is needed to cause transitions between gaits, for example from a pronk to a bound, or from a bound to a pace.

As mentioned in Section 1, the legged platform will have a coupled oscillator controller, analogous to an animal's central pattern generator. This controller will generate oscillatory patterns corresponding to various gaits in response to a command input. The platform

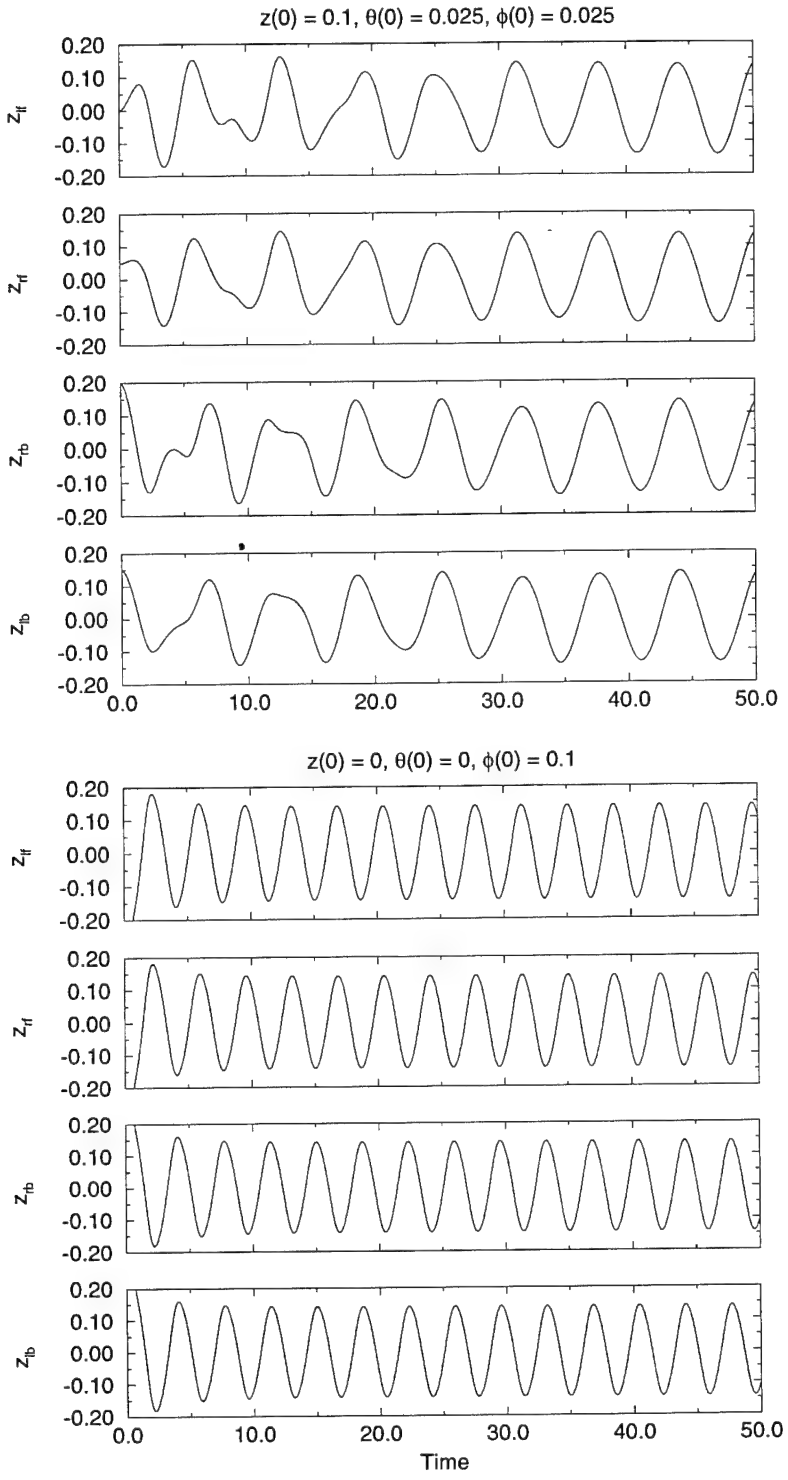

Figure 8: Vertical Oscillations of the Platform Corners. *Top:* Convergence to Pronk Pattern (case 4). *Bottom:* The Bound Pattern (case 5). Both plots are results of simulations of equations (20) – (22) with $\epsilon = 0.1$, z and θ scaled by $1/\sqrt{50}$, and ϕ scaled by $1/\sqrt{450}$. The heights are given by $z_{lf} = z - w\theta/2 - l\phi/2$, etc.

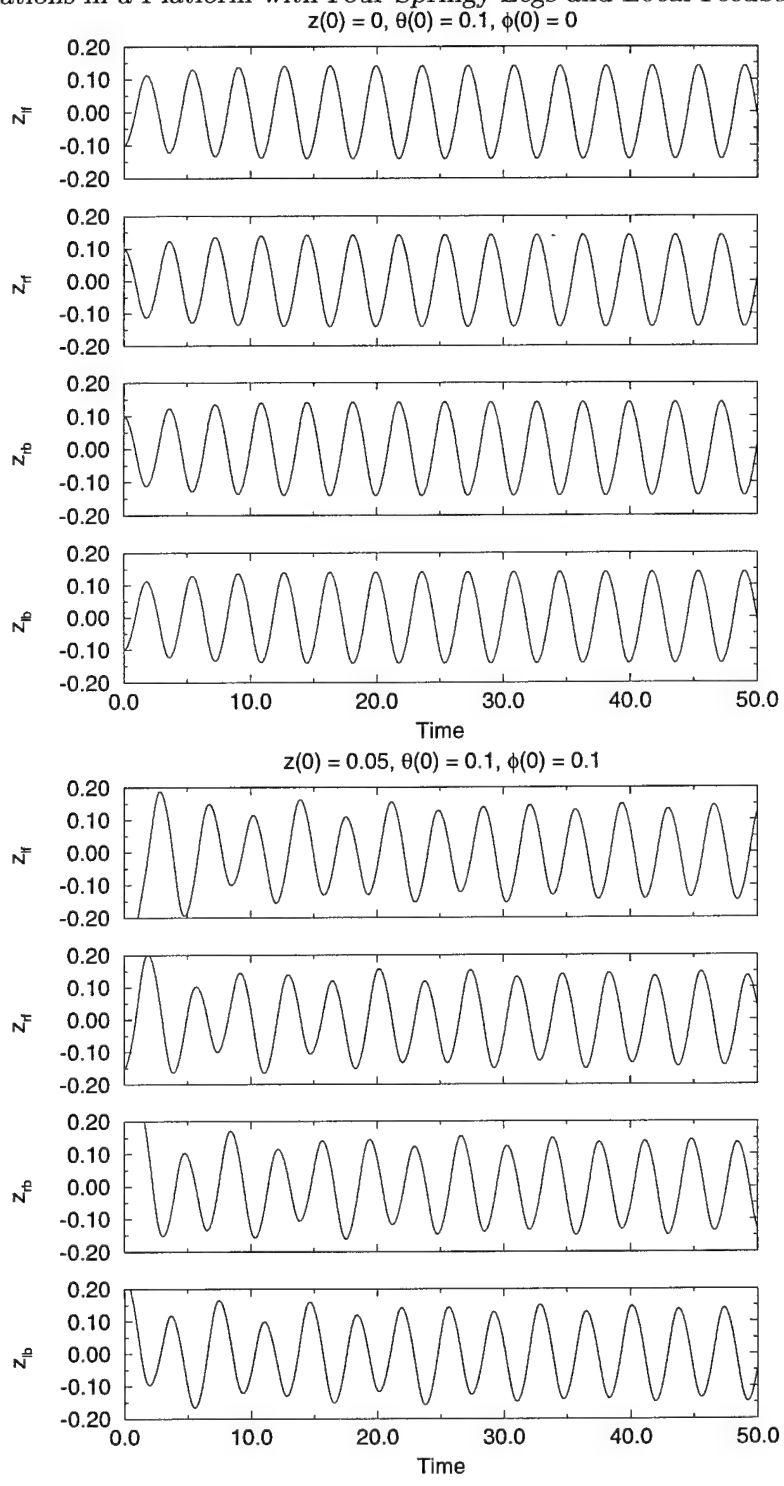

Figure 9: Vertical Oscillations of the Platform Corners. *Top:* The Pace Pattern (case 5). *Bottom:* Convergence to a Rotary Gallop Pattern (case 5). Both plots are results of simulations of equations (20) – (22) with $\epsilon = 0.1$, z and θ scaled by $1/\sqrt{50}$, and ϕ scaled by $1/\sqrt{450}$. The heights are given by $z_{lf} = z - w\theta/2 - l\phi/2$, etc.

will be coupled to the oscillator network and through this connection it is expected that the gaits mentioned earlier can be made asymptotically stable, and gait transitions can be performed. Each oscillator in the artificial CPG would be coupled to a leg's actuator as well as to other oscillators in the CPG. Note that the artificial CPG constitutes another layer of control on top of the local feedback.

In order to explore the feasibility of this approach, a few numerical experiments were performed. Equation (19) was modified by adding an additional input:

$$f_i' = (a - bz_i^2)\dot{z}_i + f_i'', \ i \in \{lf, rf, lb, rb\}$$

In future work these inputs will come from an oscillator in an artificial CPG, but for this simple study, a sinusoid at the correct frequency and phase was used.

Two numerical experiments were performed as follows:

1. *Pronk-to-bound transition:* Here, the platform was started with a pronk motion, and after 5 s the additional inputs were turned on in an attempt to perform a transition to a bound. The additional inputs were set to

$$\begin{aligned} f_{lf}'' &= f_{rf}'' = d\sin\sqrt{3}t \\ f_{lb}'' &= f_{rb}'' = -d\sin\sqrt{3}t \end{aligned}$$

   where d was made large enough to cause the transition to occur. The result is shown in Figure 10 (top).

2. *Bound-to-pace transition:* In this case, the platform was started with the bound phase relationship, and the additional inputs were turned on after 5 s as follows:

$$\begin{aligned} f_{lf}'' &= f_{lb}'' = d\sin\sqrt{3}t \\ f_{rf}'' &= f_{rb}'' = -d\sin\sqrt{3}t \end{aligned}$$

   The result is shown in Figure 10 (bottom).

These results suggest that gait transitions using a network of coupled oscillators as a controller are feasible. Future work will involve a more careful study of the artificial CPG controller.

4 Future Work

This paper has presented preliminary work on a new project, and thus there is a long list of issues that remain to be addressed. One of the first problems that will be studied next will be the selection of a new model in which the feet are allowed to leave the ground. There already exists a series of papers on the analysis of Raibert's one-legged hopper, e.g., Bühler & Koditschek (1988), Vakakis & Burdick (1990), Li & He (1990), which will likely suggest an appropriate model. Another important problem to be considered soon will be the effect of varying the masses and inertias. When the robot is constructed it is unlikely that a uniformly distributed mass will be achievable (or even desirable) as was assumed in this study. The analysis in this paper suggests that various bifurcations will occur as

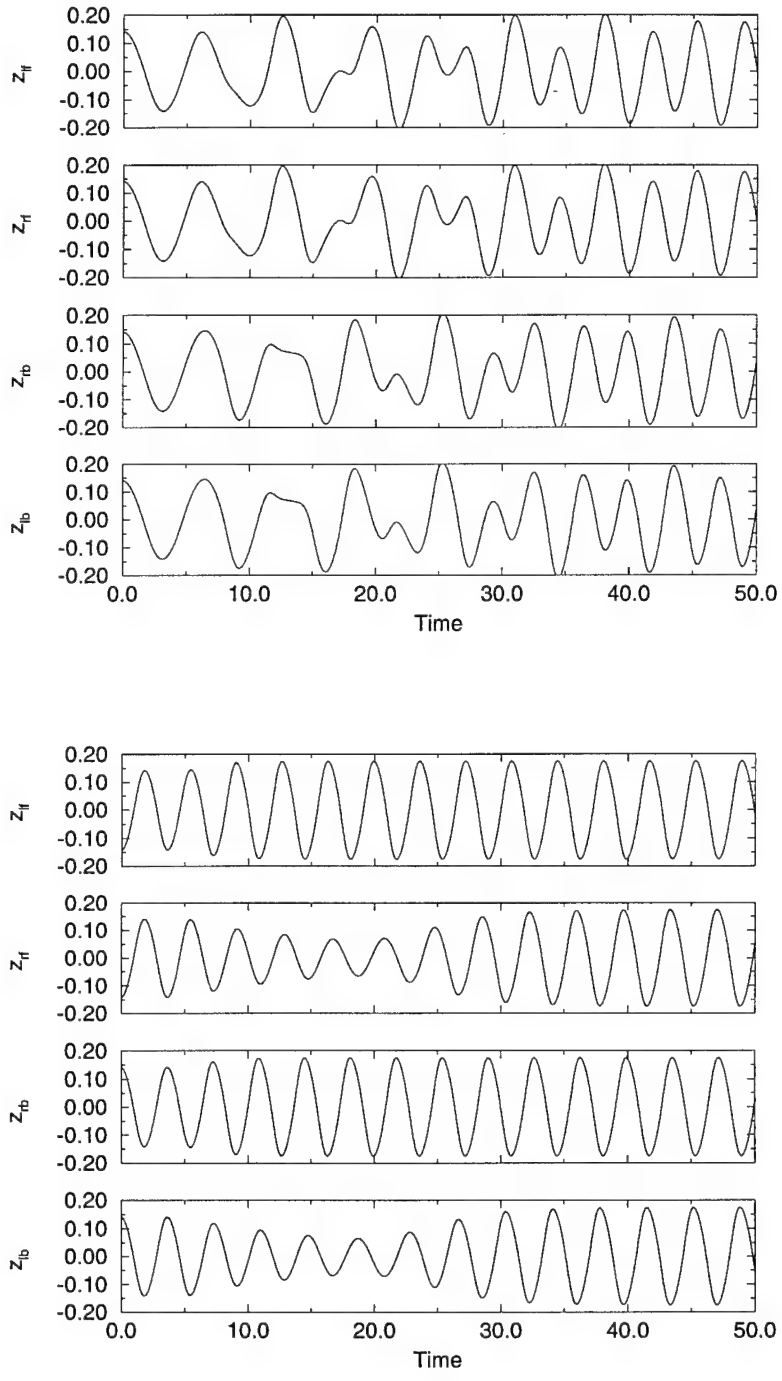

Figure 10: Vertical Oscillations of the Platform Corners. *Top:* Transition from a Pronk to a Bound. *Bottom:* Transition from a Bound to a Pace.

the masses and distributions are varied. Next, although it appears that an artificial central pattern generator should be capable of further stabilizing the various gaits and performing gait transitions, an appropriate coupled oscillator network still needs to be chosen and analyzed. The networks discussed in Collins & Stewart (1993) and Collins & Richmond (1994) are a likely place to start. Forward motion needs to be considered at some point, and last (but not least), a four-legged robot which makes use of these principles needs to be designed and constructed.

5 Conclusions

Current nonlinear control theory does not seem to be well-suited to the legged robot control problem. However, inspiration from nature and coupled oscillator theory suggest some exciting new approaches to the problem. Progress has been made in understanding the animal central pattern generator through coupled oscillator theory, but so far very few researchers have considered modeling the coupling of CPGs to animal musculoskeletal dynamics. This idea has much potential as an approach for controlling legged robots. In this paper a four-legged platform with simple local feedback was studied. This platform was shown to have stable oscillations corresponding to the pronk, bound, pace, and rotary gallop gaits. Furthermore, numerical experiments demonstrated the feasibility of using an artificial CPG to further stabilize the gaits and to cause transitions between gaits.

Acknowledgments

The author is grateful to Joel Burdick for introducing him to coupled oscillator research. The author also appreciated the opportunity to present preliminary ideas along these lines to Marc Raibert and his Leg Lab group.

References

Alexander, R. M. (1984), 'The gaits of bipedal and quadrupedal animals', *International Journal of Robotics Research* **3**(2), 49–59.

Ayers, J. & Crisman, J. (1993), Lobster walking as a model for an omnidirectional robotic ambulation architecture, *in* R. D. Beer, R. E. Ritzmann & T. McKenna, eds, 'Biological Neural Networks in Invertebrate Neuroethology and Robotics', Academic Press, chapter 13.

Bay, J. S. & Hemami, H. (1987), 'Modeling of a neural pattern generator with coupled nonlinear oscillators', *IEEE Transactions on Biomedical Engineering* **BME-34**(4), 297–306.

Bühler, M. & Koditschek, D. E. (1988), Analysis of a simplified hopping robot, *in* 'Proceedings of the 1988 IEEE International Conference on Robotics and Automation', pp. 817–819.

Chiel, H. J., Beer, R. D. & Sterling, L. S. (1989), Heterogeneous neural networks for adaptive behavior in dynamic environments, *in* D. S. Touretzky, ed., 'Advances in Neural Information Processing Systems I', Morgan Kaufmann Publishers, pp. 577–585.

Chiel, H. J., Beer, R. D., Quinn, R. D. & Espenschied, K. S. (1992), 'Robustness of a distributed neural network controller for locomotion in a hexapod robot', *IEEE Transactions on Robotics and Automation* **8**(3), 293–303.

Collins, J. J. & Richmond, S. A. (1994), 'Hard-wired central pattern generators for quadrupedal locomotion', *Biological Cybernetics* **71**, 375–385.

Collins, J. J. & Stewart, I. N. (1993), 'Coupled nonlinear oscillators and the symmetries of animal gaits', *Journal of Nonlinear Science* **3**, 349–392.

Full, R. J. (1993), Integration of individual leg dynamics with whole body movement in arthropod locomotion, *in* R. D. Beer, R. E. Ritzmann & T. McKenna, eds, 'Biological Neural Networks in Invertebrate Neuroethology and Robotics', Academic Press, chapter 1.

Gordon, J. (1991), Spinal mechanisms of motor coordination, *in* E. R. Kandel, J. H. Schwartz & T. M. Jessel, eds, 'Principles of Neural Science', 3rd edn, Elsevier, chapter 38.

Guckenheimer, J. & Holmes, P. (1983), *Nonlinear Oscillations, Dynamical Systems, and Bifurcations of Vector Fields*, Springer-Verlag.

Hale, J. K. (1980), *Ordinary Differential Equations*, Robert E. Krieger Publishing Company.

Hildebrand, M. (1989), 'The quadrupedal gaits of vertebrates', *BioScience* **39**(11), 766–775.

Katoh, R. & Mori, M. (1984), 'Control method of biped locomotion giving asymptotic stability of trajectory', *Automatica* **20**(4), 405–414.

Kopell, N. (1988), Toward a theory of modelling central pattern generators, *in* A. H. Cohen, S. Rossignol & S. Grillner, eds, 'Neural Control of Rhythmic Movements in Vertebrates', Wiley, chapter 10.

Lewis, M. A., Fagg, A. H. & Solidum, A. (1992), Genetic programming approach to the construction of a neural network for control of a walking robot, *in* 'Proceedings of the 1992 IEEE International Conference on Robotics and Automation', pp. 2618–2623.

Li, Z. & He, J. (1990), An energy perturbation approach to limit cycle analysis in legged locomotion systems, *in* 'Proceedings of the 29th IEEE Conference on Decision and Control', pp. 1989–1994.

Marvin, D. J. (1992), Coordination of the walking stick insect using a system of nonlinear coupled oscillators, Master's thesis, University of Maryland.

Mishra, S. (1993), Control of locomotion using coupled oscillators, Master's thesis, University of Maryland.

Pearson, K. (1976), 'The control of walking', *Scientific American* **235**(6), 72–86.

Pearson, K. G. & Duysens, J. (1976), Function of segmental reflexes in the control of stepping in cockroaches and cats, *in* R. M. Herman, S. Grillner, P. S. G. Stein & D. G. Stuart, eds, 'Neural Control of Locomotion', Plenum Press, New York, pp. 519–537.

Raibert, M. H. (1986), *Legged Robots That Balance*, MIT Press.

Raibert, M. H. (1990), 'Trotting, pacing, and bounding by a quadruped robot', *Journal of Biomechanics* **23**, 79–98. Supplement 1.

Rand, R. H., Cohen, A. H. & Holmes, P. J. (1988), Systems of coupled oscillators as models of central pattern generators, *in* A. H. Cohen, S. Rossignol & S. Grillner, eds, 'Neural Control of Rhythmic Movements in Vertebrates', Wiley, chapter 9.

Song, S.-M. & Waldron, K. J. (1989), *Machines That Walk*, MIT Press.

Strogatz, S. H. & Stewart, I. (1993), 'Coupled oscillators and biological synchronization', *Scientific American* **269**(12), 102–109.

Vakakis, A. F. & Burdick, J. W. (1990), Chaotic motions in the dynamics of a hopping robot, *in* 'Proceedings of the 1990 IEEE International Conference on Robotics and Automation', pp. 1464–1469.

Design of a Robot Leg with Elastic Energy Storage, Comparison to Biology, and Preliminary Experimental Results[1]

Matthew D. Berkemeier
Kamal V. Desai

DRAFT — Not in Final Form.

August 14, 1995

[1]supported by ONR grant no. N00014-95-1-0560.

1 Introduction

Research on artificial legged locomotion has the potential for producing vehicles and mobile robots which are capable of easily crossing rocky terrain, climbing or jumping over large obstacles, and agilely maneuvering in tight surroundings. Specific examples of needs for these capabilities include Mars exploration, military assault or transport, underwater exploration, and hazardous site inspection. A further benefit to research in this area is the insight it gives into the animal locomotory control system.

Our ultimate goal is to construct a quadruped robot which will be capable of a number of running gaits such as the pronk, pace, bound, and gallop. Motivated by the work of researchers in mathematical biology, such as Collins & Stewart (1993) and Rand, Cohen & Holmes (1988), it will be controlled by a network of coupled oscillators. Previously we have shown in Berkemeier (1995) that a platform suspended by four springy legs and having simple, local "reflex functions" will naturally tend toward particular oscillation patterns corresponding to animal gaits.

In this paper we focus on the specifics of designing a suitable leg for our robot. We only address the problem of achieving energetic vertical oscillations. Horizontal motions will be dealt with at a future date.

McMahon (1985) and McMahon, Valiant & Fredrick (1987) have demonstrated the utility of modeling human and animal legs by springs and masses during running gaits. Raibert (1986) and Raibert (1990) has shown that this can also form a simple but powerful approach to legged robot design and control. Results of these researchers suggest that it is possible to design quadrupedal robot legs in isolation without having to consider the dynamics of the whole robot. Thus, our approach in this paper will also be based on simple spring and mass models. However, we will present a novel design which, to the best of our knowledge, has not been attempted before. Our design is "biologically-styled" in that it contains a foot which is actuated through springy tendons. We rely on mechanical energy storage and recovery to achieve sufficiently large vertical oscillations. We also present preliminary results which demonstrate that our leg is on the verge of hopping.

2 Leg Design

We begin by describing design choices for the simplest leg model (basically just a mass on top of a massless spring). Next, design choices for a more biologically-styled leg are described. Lastly, we present our final design.

2.1 Linear Leg Model

Consider the simple leg model in Figure 1. The equations of motion are given in Appendix A as equations (2) and (3). Also given are formulas for minimum and maximum heights (5 and 6) as well as time on ground and in air (8 and 9). These formulas all depend on two design parameters: n and ω.

n determines the amplitude/shape of the hopping cycle trajectory (Figure 11). There is a direct correspondence between n and the Groucho number, a dimensionless parameter introduced in McMahon et al. (1987). They found that the Groucho number for human

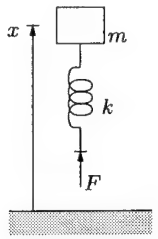

Figure 1: A Simple Leg Model

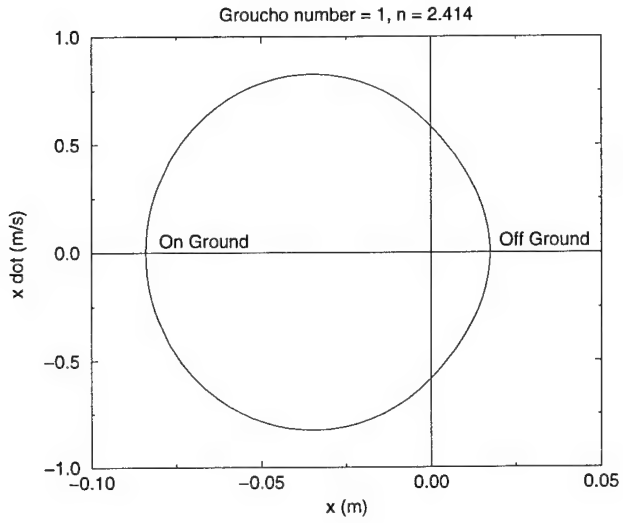

Figure 2: Hopping Phase Plot for a Groucho Number of One. Takeoff occurs when $x = 0$. $\omega = 16.78$ rad/s was assumed to generate the plot.

runners was approximately one. On the other hand, the quadruped of Raibert (1990) had a Groucho number of 2.6 for trotting and 1.29 for bounding. We have chosen a Groucho number of one to correspond to biological systems. From equation (7) this gives $n = 2.414$. Figure 2 shows a phase plot of the hopping motion. For this value of n the hopping height is less than the spring compression, and the time in the air is less than the ground contact time.

The other important parameter to be chosen is ω, the resonant frequency of the leg while on the ground. The value of ω determines two numbers of importance to us: the maximum compression of the spring and the hopping frequency. The maximum spring compression will typically be bounded due to joint/spring limits. The hopping frequency must be sufficiently slow due to limited computer and actuator bandwidths. A tradeoff is present here: the slower the hopping frequency, the larger the spring compression. Figure 3 illustrates this tradeoff and was drawn using equations from Appendix A. We decided on a hopping frequency of 2.5 Hz. The reader may verify that it is possible for humans to hop on one foot at this frequency. This gave $\omega = 16.78$ rad/s and a maximum spring compression

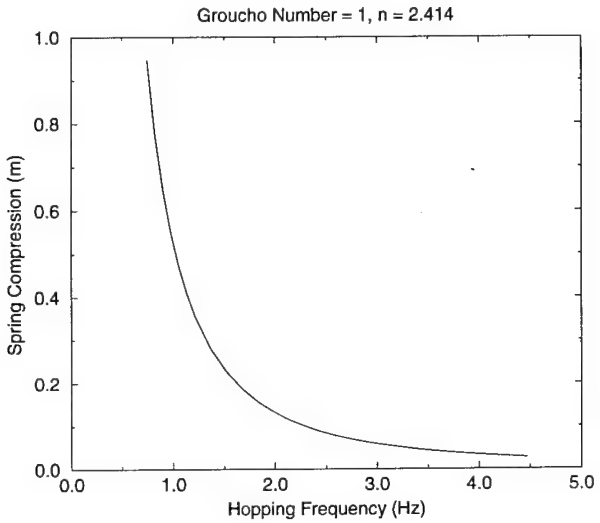

Figure 3: Tradeoff Between Hopping Frequency and Maximum Spring Compression.

Parameter	Value	Unit
Groucho Number	1	—
n	2.414	—
ω	16.78	rad/s
$k/m = \omega^2$	281.6	N/m/kg
Hopping Frequency	2.5	Hz
Max. Spring Compression	0.084	m
Avg. Power During Contact	1.214	W/kg
Min. Actuator Force	23.66	N/kg

Table 1: Design Parameters for the Linear Leg

of $x = 8.4$ cm.

Next, we consider the actuator requirements. For the chosen parameters, the energy per unit mass of the hopping cycle, E, is 0.3411 J/kg (equation (4)), and the contact time is 0.2809 s (equation (8)). The ratio of these two numbers is the average power per mass required to start the leg from rest during the contact period and is $P = 1.214$ W/kg. Our actuator choice should be able to supply a substantial fraction of this power (due to dissipative energy losses such as friction and impact). The minimum force required from the actuator can be calculated from equation (10). Plugging in gives $f = 23.66$ N/kg.

Table 1 summarizes our design parameter choices for the simple linear leg model.

2.2 A More Biologically-Styled Leg

In biological systems several muscles work together in groups of opposing pairs to rotate a joint. A system with such a high degree of redundancy may be difficult to control (from a control theorist's perspective) but offers many advantages such as fault-tolerance and reduced requirements of precision and accuracy in the individual components. Muscles are also extremely lightweight relative to the force they can generate. Currently, there does not exist a reliable, easy-to-use actuator with the mechanical properties of muscle, although this is an active research area. Hannaford & Winters (1990) provide a comparison between man-made and biological actuators. Muscles are connected in series with tendons. It is well-known that tendons are capable of providing elastic energy storage (Alexander 1984).

We have chosen to use a DC motor instead of a more muscle-like actuator. DC motors are very reliable, clean, well-understood, and easy to use. Not many researchers have utilized DC motors for hopping or running robots. An exception is Papantoniou (1991) who constructed a one-legged robot powered by an electric motor which hopped in a manner similar to Raibert's robot. Since DC motors are very heavy and bulky for the force they produce, it is not feasible to have many acting in parallel to control a joint if we wish to come close to producing biological-like motions. It is feasible however, to attach elastic elements such as steel springs in series with a DC motor to mimic the biological tendon. Figure 4 shows a design for actuating the ankle joint of our robot. The rotation of the pulley at the top simultaneously draws one cable up and allows the other to move down. To the best of our knowledge, no one else has ever tested such a design. The closest example is the work of Lee & Raibert (1991). However, in this case, instead of having compliant tendons, the foot itself flexed.

Although seemingly quite different from the linear leg models in Figures 1 and 10, the biologically-styled design is actually similar, and it is possible to transform the numbers for the linear design to relevant parameters for this design (This is most easily done by ignoring, for now, the fact that the transformations are dependent on the configuration of the biologically-styled leg). Notice that the biologically-styled leg has an actuator in series with an elastic member just like the linear leg. Assume initially that the motor shaft is fixed. Also, assume that both tendons are always in tension. Straightforward calculations then yield the relationship between the effective stiffness of the leg, $k_{\text{eff}} = f/x$ and the tendon stiffness, k, as

$$k_{\text{eff}} = 2k\left(\frac{\rho}{d}\right)^2 \tag{1}$$

Also, the assumption that both tendons are always in tension effectively halves the maximum x displacement that would be available if only one spring were used. Displacements and forces clearly map as

$$\begin{aligned} x &= \theta r\left(\frac{d}{\rho}\right) \\ f &= \frac{\tau}{r}\left(\frac{\rho}{d}\right) \end{aligned}$$

We have chosen the ratio $d/\rho = 5$ to roughly correspond to biology. Also, $r = 1.27$ cm was a convenient value for our leg. This yields the new parameters in Table 2. The maximum

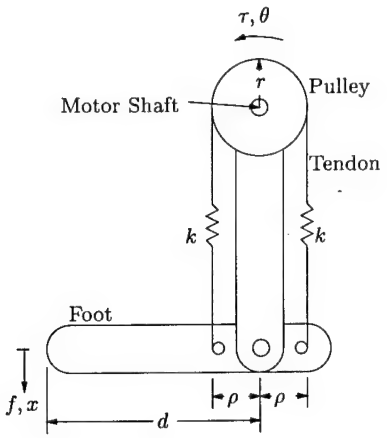

Figure 4: A More Biologically-Styled Leg Design

Parameter	Value	Unit
Groucho Number	1	—
n	2.414	—
ω	16.78	rad/s
$k_{\text{eff}}/m = \omega^2$	281.6	N/m/kg
d/ρ	5	—
r	0.0127	m
k/m	3520	N/m/kg
Hopping Frequency	2.5	Hz
Max. Spring Extension	0.0336	m
Avg. Power During Contact	1.214	W/kg
Min. Actuator Torque	1.502	N-m/kg

Table 2: Design Parameters for the Biologically-Styled Leg.

spring extension in the table includes the necessary amount required for pretension as explained above.

2.3 The Final Design

Having determined the basic parameters for our leg, the next step was to make specific choices for the components and then assemble the leg. We chose to make the leg out of aluminum. Aluminum is very strong for its weight and is easy to machine. These two qualities make it a popular material for robot construction. We chose a DC motor with rare earth magnets from Maxon (model RE025-055-38EBA201A), an integral gearhead (Maxon model 2932.703-0181.0-000), and an integral HP encoder (model HEDS 5010). Bearings, shafts, etc. were purchased from PIC manufacturing, and the steel cable tendons were purchased from McMaster-Carr Supply Company. We also used a pair of bevel gears

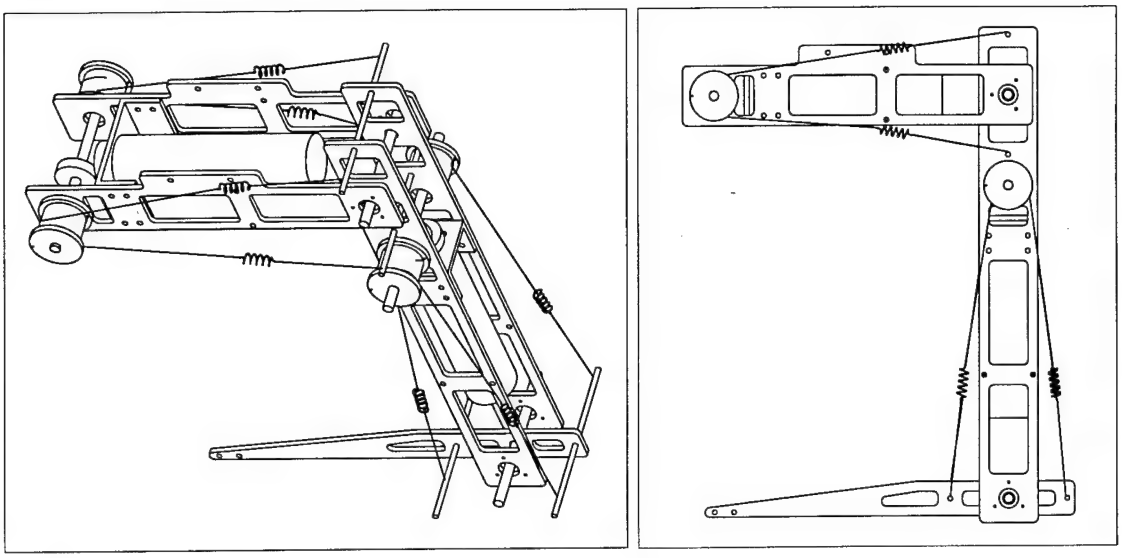

Figure 5: CAD Drawings of the Quadruped Leg. *Left:* Isometric view. *Right:* Side View.

purchased from Stock Drive Products to effect a 90° change of the axis of rotation. Steel springs for the tendons were purchased from Hardware Products Company, a local business. Our design is shown in Figure 5. In anticipation of the next step, our current design includes a tendon-driven hip joint, although we are not yet prepared to discuss analysis of this joint. Figure 6 is a photograph of our leg.

In order to test the leg's performance without constructing the entire robot, we mounted it to an instrumented boom as described in Section 4. The boom plus attached circuit boards and wires weighed roughly 1.2 kg while the leg (including one motor) weighed roughly 1.1 kg, bringing the total weight to 2.3 kg. This total mass value was used to compute the absolute parameter values associated with the relative values given in Table 2.

Table 3 compares design and actual values for our leg. k is the spring constant for the individual springs in the tendons. Notice that our design in Figure 5 has a total of four springs instead of the two in Figure 4. This adds another factor of two to the formula given in equation (1), which was used to calculate the k_{eff} value in the table. The maximum spring extension in the table includes the necessary amount required for pretension as explained previously. The fact that our current springs do not meet the design goal was due to an oversight on our part and will be remedied. It was a limiting factor in our experimental results. The current average power during contact value was based on our motor's output of 0.0303 N-m $\times$ 418.9 rad/s = 12.7 W multiplied by a conservative efficiency factor of 50% to include efficiencies of the integral gearhead, bevel gears, bearings, and tendons. The current minimum actuator torque value was based on the maximum continuous torque rating of the motor (0.0303 N-m) multiplied by the gear ratio (181:1) and by a conservative factor of 50%. The Groucho and n values for the current design were based on experimental results in Section 4. From Table 3 it is clear that, aside from the maximum spring extension, our current implementation has indeed met our design goals. With longer springs, we expect to be able to also reach the desired Groucho number.

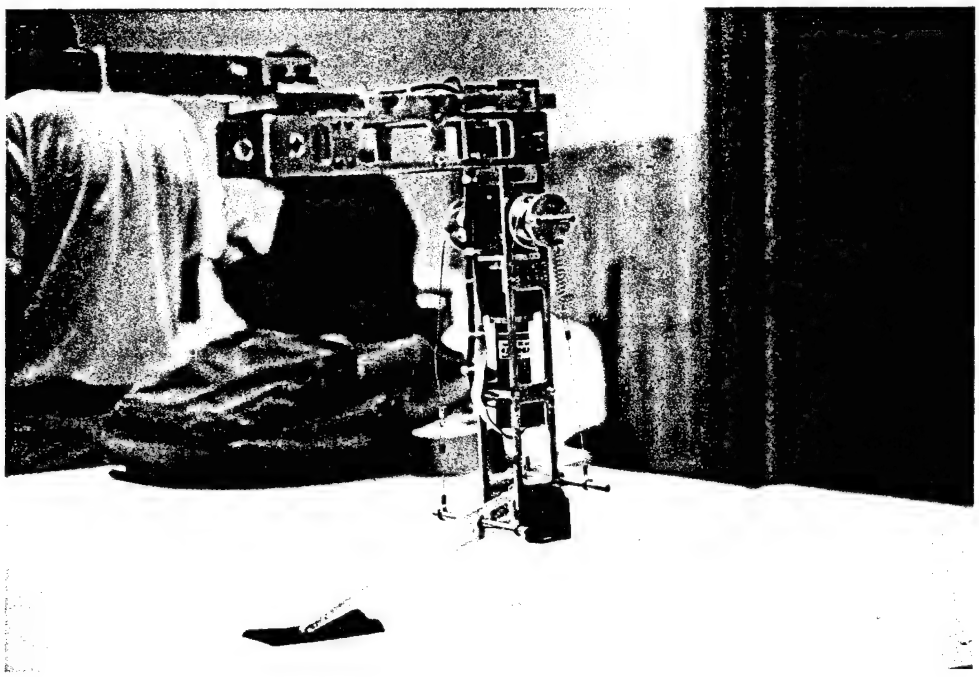

Figure 6: Photograph of the Quadruped Leg.

Parameter	Design Value	Current Value	Unit
m	—	2.3	kg
Groucho Number	1	≈ 0	—
n	2.414	≈ 2	—
k	4048	4030	N/m
k_{eff}	647.7	645	N/m
$\omega = \sqrt{k_{\text{eff}}/m}$	16.8	16.8	rad/s
d/ρ	5	5	—
r	0.0127	0.0127	m
Hopping Frequency	2.5	2.5	Hz
Max. Spring Extension	0.0337	0.0211	m
Avg. Power During Contact	2.80	6.35	W
Min. Actuator Torque	1.50	2.74	N-m

Table 3: Comparison of Design and Actual Parameter Values. See text for an explanation.

Simplified Muscle Group	Original Muscle Group
a	RF, IP, SART (6, 7, 8)
b	BPST, BASM (3, 5)
c	PTF (9)
d	GAST, FLFH, SOL (2, 10, 1)

Table 4: Contents of the Four Muscle Groups.

3 Comparison to a Cat's Hindlimb

Animals provide a benchmark against which our leg, and eventually our quadrupedal robot, may be compared. The engineered mechanism will almost always come out the loser in such a performance comparison, but there is a good possibility that insight can be gained into better ways to engineer robots and into better understanding of animal locomotion.

Cats are popular subjects in laboratory tests, and there is clearly much that those building legged robots can learn from them. Cats are extremely graceful, powerful, and efficient during locomotion. These are also desirable qualities for a legged robot.

3.1 Structural Comparison

Figure 7, part a), shows the anatomical arrangement the muscles in the cat hindlimb along with the skeleton. The four major bones are the pelvis, thigh, shank, and foot. Based on the work of He, Levine & Loeb (1991), muscles performing similar functions have been lumped together to form ten groups. For the reader's convenience, we have duplicated their groupings in Appendix B

If the knee joint is locked, so that the leg now only has two joints, then the leg can be simplified as shown in Figure 7, part b). This allows us to make a reasonable comparison to our robot leg. The ten muscle groups have been further simplified into four muscle groups. Table 4 shows the composition of the new groups. Note that extensor 4 (VAST), which acts over the knee joint, is now assumed to be a part of the shank in our simplified representation and will be ignored.

[This section is incomplete.]

4 Preliminary Experimental Results

As mentioned earlier, we have set up an instrumented boom for testing the individual legs of our quadruped. We felt this to be an important step since it will allow us to optimize our design before building all of the legs.

The computer we are using for robot control is a Motorola MVME167 single-board computer which is housed in a VMEbus card cage. We are running LynxOS on the computer, which is a real-time UNIX. In addition to the computer, we have a number of VMEbus cards for I/O including A/D, D/A, parallel I/O, and encoder boards. Communication with

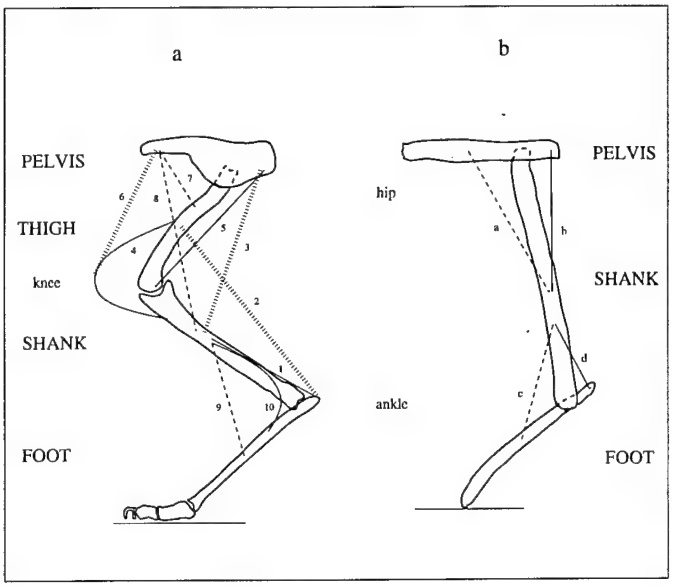

Figure 7: Cat Hindlimb: a) Simplified Representation of the Anatomical Arrangement of the Muscles. The solid lines represent the extensor muscles, while the dashed lines are the flexors. The dotted lines are those that act over two joints, and are thus both flexors and extensors. For example, muscle group 2, comprising the Medial Gastrocnemius (MG) and the Lateral Gastrocnemius (LG), flexes over the knee joint while extending at the ankle joint. Based on He et al. (1991). b) An Extremely Simplified Version. This version can be easily compared to our robot leg.

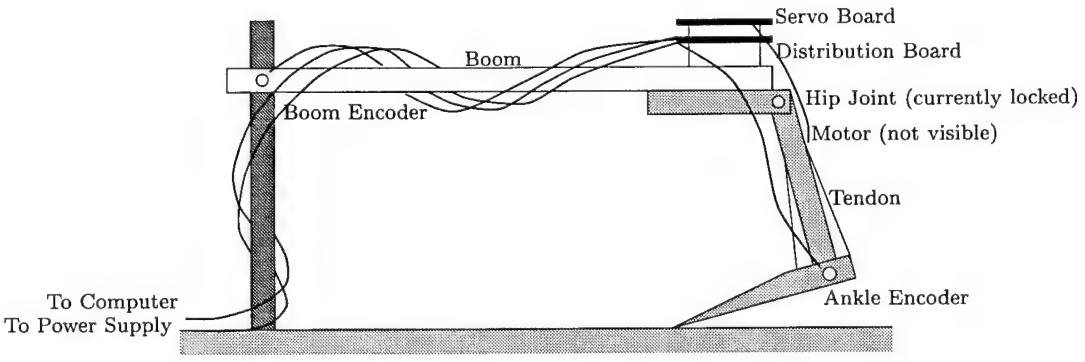

Figure 8: Leg Testing System

these boards is facilitated by device drivers, which we have been writing ourselves. Figure 8 shows the testing system we have built.

The servo board shown in Figure 8 is a PID controller in hardware. It was built around the National Semiconductor LM628 Precision Motion Controller chip. It allows us to control desired position or velocites of the motor without having to do the PID calculations in software. As a first, easy step in evaluating the leg's performance, we commanded periodic motor position trajectories at 2.5 Hz, the desired hopping frequency. For some trials the foot left the ground for short instances, but mostly it stayed on the ground. We felt this was due to use of springs with insufficient maximum stretch, as documented in Table 3. On the other hand it was quite clear that we were driving the leg at close to resonance, as the motion was quite energetic despite relatively small input amplitudes. Finding the exact resonance frequency (which we have not attempted yet) would increase the amplitude of the oscillations even more.

Figure 9 shows data collected from our boom encoder. Peak-to-peak oscillations were roughly 7.2 cm (Unfortunately, the resolution of our system was only 0.314 cm.) This was achieved by using motor oscillations which, if not assisted by energy storage and recovery, produced only 1.65 cm oscillations of the foot. Thus, the gain of the system for this frequency was about 4.4 making it clear that we were driving the leg at near resonance.

Did we come close to hopping for this particular trial? Based on the peak-to-peak oscillation value of 7.2 cm, the formulas in Appendix A yield a Groucho number of 0.273 and $n = 2.04$, which would suggest that the leg was hopping, but only just barely. Of course, it is quite likely that due to our lack of resolution in measuring the leg height, the oscillations do not have an amplitude of 7.2 cm but something less. In any case, the numbers suggest that the leg was at least on the verge of hopping in this particular trial. With springs having a higher maximum extension, we expect to be able to easily make the leg hop using this approach. We could also increase the oscillation amplitudes by finding the exact resonance frequency of the leg. An even better way to produce these oscillations (and what we plan to use for the quadruped robot) would be to use feedback from the ankle encoder (Figure 8). Then we could have the foot push down when the leg was on its way up, and have the foot pull up when the leg was on its way down. We hope to implement such an energy pumping strategy in the near future. This also should improve our results.

5 Conclusions

[This section is incomplete.]

Acknowledgments

The authors are grateful to Ed Nicolson for advice on control software and to Sameer Madenshetty for guidance on mechanical design. Kevin Chu's assistance on this project was greatly appreciated.

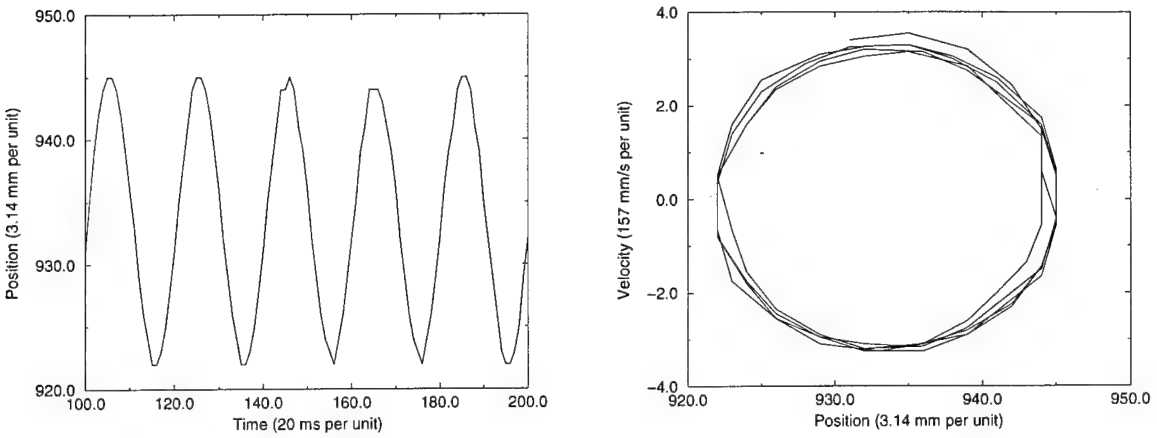

Figure 9: Preliminary Experimental Data.

References

Alexander, R. M. (1984), 'The gaits of bipedal and quadrupedal animals', *International Journal of Robotics Research* **3**(2), 49–59.

Berkemeier, M. D. (1995), Coupled oscillations in a platform with four springy legs and local feedback, *in* 'Proceedings of the 34th IEEE Conference on Decision and Control'. To appear.

Collins, J. J. & Stewart, I. N. (1993), 'Coupled nonlinear oscillators and the symmetries of animal gaits', *Journal of Nonlinear Science* **3**, 349–392.

Hannaford, B. & Winters, J. (1990), Actuator properties and movement control: Biological and technological models, *in* J. M. Winters & S. L.-Y. Woo, eds, 'Multiple Muscle Systems: Biomechanics and Movement Organization', Springer-Verlag, chapter 7, pp. 101–120.

He, J., Levine, W. & Loeb, G. (1991), 'Feedback gains for correcting small perturbations to standing posture', *IEEE Transactions on Automatic Control* **36**(3), 322–332.

Lee, W. & Raibert, M. H. (1991), Control of hoof rolling in an articulated leg, *in* 'Proceedings of the 1991 IEEE International Conference on Robotics and Automation', pp. 1386–1391.

McMahon, T. A. (1985), 'The role of compliance in mammalian running gaits', *Journal of Experimental Biology* **115**, 263–282.

McMahon, T. A., Valiant, G. & Fredrick, E. C. (1987), 'Groucho running', *Journal of Applied Physiology* **62**(6), 2326–2337.

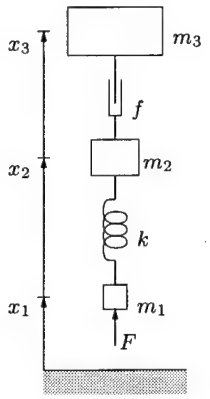

Figure 10: Notation for Leg Model

Papantoniou, K. V. (1991), Electromechanical design for an electrically powered, actively balanced one leg planar robot, *in* 'Proceedings of the 1991 IEEE/RSJ International Conference on Intelligent Robots and Systems', pp. 1553–1560.

Raibert, M. H. (1986), *Legged Robots That Balance*, MIT Press.

Raibert, M. H. (1990), 'Trotting, pacing, and bounding by a quadruped robot', *Journal of Biomechanics* **23**, 79–98. Supplement 1.

Rand, R. H., Cohen, A. H. & Holmes, P. J. (1988), Systems of coupled oscillators as models of central pattern generators, *in* A. H. Cohen, S. Rossignol & S. Grillner, eds, 'Neural Control of Rhythmic Movements in Vertebrates', Wiley, chapter 9.

A Linear Leg Model Calculations

In this appendix we give the details of the equations for our linear leg model. The derivations are straightforward but are included for the reader's convenience.

A.1 The Linear Leg Model

Figure 10 shows the general linear model used in this paper. Point masses are assumed. An actuator supplies a force f between masses m_2 and m_3. A linear spring with stiffness k is located between masses m_2 and m_1. F is the ground reaction force. Notice that x_2 and x_3 are relative positions. m_2 models the spring mass and the portion of the actuator mass attached to the spring. m_1 models the unsprung mass of the foot. m_3 models the remaining leg mass including the portion of the actuator mass fixed to it.

The equations of motion for the model are given by

$$\begin{aligned} m_3(\ddot{x}_1 + \ddot{x}_2 + \ddot{x}_3) &= f - m_3 g \\ m_2(\ddot{x}_1 + \ddot{x}_2) &= -f - m_2 g - k x_2 \\ m_1 \ddot{x}_1 &= F - m_1 g + k x_2 \end{aligned}$$

Various simplifications of this model may be assumed. First, the system will be studied with the foot on the ground ($x_1 = 0$). Also, initially, the case where the actuator is locked is studied so that x_3 is a constant. It will be convenient to choose $x_3 = 0$. Thus, m_2 and m_3 can be lumped together as $m = m_2 + m_3$, and for convenience let $x = x_2$. Assuming also that $m_1 = 0$ gives the equations

$$m\ddot{x} + mg + kx = 0 \tag{2}$$

$$F = -kx \tag{3}$$

Notice that $F \geq 0$ since the ground cannot pull down on the foot. Note also that $F = 0$ implies $x = 0$ and $\ddot{x} = -g$. This latter equation, of course, is the equation of motion while the the foot is off the ground.

The change of variable

$$y = x + \frac{mg}{k} = x + \frac{g}{\omega^2}$$

where $\omega = \sqrt{k/m}$ is the resonant frequency of the leg on the ground gives a simple harmonic oscillator equation

$$\ddot{y} + \omega^2 y = 0$$

with constant of motion, E, the energy per unit mass:

$$E = \frac{1}{2}\dot{y}^2 + \frac{1}{2}\omega^2 y^2$$

It turns out to be convenient to choose an initial condition of the form ($x = -ng/\omega^2, \dot{x} = 0$) with $n > 2$ (For $0 \leq n \leq 2$ the leg never leaves the ground). The energy per unit mass of this state is

$$E = \frac{1}{2}(n-1)^2\frac{g^2}{\omega^2} \tag{4}$$

This allows us to solve for the velocity of the leg at takeoff. Recall that at takeoff, $x = 0$, so

$$\frac{1}{2}(n-1)^2\frac{g^2}{\omega^2} = \frac{1}{2}\dot{x}^2 + \frac{1}{2}\frac{g^2}{\omega^2}$$

This gives the velocity at takeoff as

$$\dot{x}^2 = n(n-2)\frac{g^2}{\omega^2}$$

Since the hopping height is given by $\dot{x}^2/(2g)$, the leg will reach a height of

$$\frac{n(n-2)}{2}\frac{g}{\omega^2}, \; n > 2$$

To summarize, then, the two extremes of the leg height are given by

minimum:

$$x = -n\frac{g}{\omega^2} \tag{5}$$

maximum:

$$x = \frac{n(n-2)}{2}\frac{g}{\omega^2},\ n > 2 \tag{6}$$

For $n = 4$ the hopping height and maximum spring compression are equal. For $2 < n < 4$ the hopping height is less than the compression, and for $n > 4$ the hopping height is greater.

It is interesting to note that there is a direct relationship between the number n and the Groucho number introduced by McMahon et al. (1987). Since the Groucho number is given by $\dot{x}\omega/g$, where $\dot{x}$ is the touchdown/landing velocity,

$$\text{Groucho Number} = \sqrt{n(n-2)} \tag{7}$$

Next, consider the time spent on and off the ground. If $\dot{x}$ is the takeoff/landing velocity, the time spent off the ground is given by $2\dot{x}/g$ or

$$2\frac{\sqrt{n(n-2)}}{\omega}$$

To solve for the time on the ground, note that the harmonic oscillator equation

$$\ddot{y} + \omega^2 y = 0,\ y(0) = y_0,\ \dot{y}(0) = 0$$

has solution $y(t) = y_0 \cos \omega t$ or,

$$x(t) + \frac{g}{\omega^2} = \left(x_0 + \frac{g}{\omega^2}\right)\cos \omega t$$

Since $x_0 = -ng/\omega^2$,

$$x(t) = -\frac{g}{\omega^2}((n-1)\cos \omega t + 1)$$

Setting the above equation to 0 since that is where takeoff occurs yields

$$t = \frac{1}{\omega}\cos^{-1}\left(-\frac{1}{n-1}\right)$$

which, of course, is half the time on the ground. Thus, to summarize,

time on ground:

$$\frac{2}{\omega}\cos^{-1}\left(-\frac{1}{n-1}\right) \tag{8}$$

time off ground:

$$\frac{2}{\omega}\sqrt{n(n-2)},\ n > 2 \tag{9}$$

For $n \approx 3.262$ the time on the ground and in the air are equal. For $2 < n < 3.262$ the time in the air is less than the time on the ground. For $n > 3.262$, the time in the air is greater.

Equations (5), (6), (8), and (9) are the main equations used for the design. The two free variables are n and ω. Figure 11 shows the phase space trajectories for several values of n.

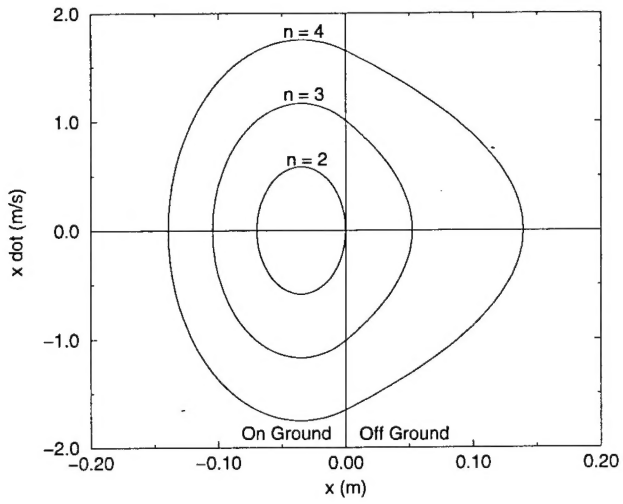

Figure 11: Hopping Phase Space Trajectories. For all three $\omega = 16.78$ rad/s. Takeoff occurs when $x = 0$.

A.2 Actuator Considerations

The next step is to consider the requirements the design places on the actuator. Recall that the energy per mass of the hopping cycle is given by equation (4). The only time the actuator can add energy to the system is when the foot is on the ground. A useful relation is the energy per contact time per unit mass. One can think of this as the average power required to start the leg from rest during its contact period. This is given by the ratio of equations (4) and (8). Now, of course, the actuator does not need to supply all this power since the system tends to conserve mechanical energy. However, due to dissipative effects such as impacts and friction, etc., it may have to supply a substantial fraction of it. One may choose a conservative fraction to use in the design such as 10, 25, or 50%.

Besides power, the maximum force required of the actuator is important to know. It is now necessary to return to the more general model originally described. If it is assumed that $m_2 \approx 0 \Rightarrow m_3 \approx m$, then the actuator force is simply

$$f = -kx$$

Recall that the minimum height of the leg is given by $-ng/\omega^2$. So, the actuator must be capable of supplying at least

$$f = nmg \tag{10}$$

B Ten Major Muscle Groups of the Cat Hindlimb

He et al. (1991) lumped muscles of the cat hindlimb which performed similar functions into ten distinct groups. We repeat their groupings in this paper for the reader's convenience in Table 5. The group numbers in the table refer to the numbers in Figure 7.

Group Number	Group Name	Muscles
1	SOL	SOL, PLA
2	GAST	LG, MG
3	BPST	BFP, ST, GRA, TS
4	VAST	VI, VM, VL
5	BASM	BFA, SMA, SMP, AF, CF, QF, TFP
6	RF	RF, TFA, SAA
7	IP	IP
8	SART	SAM
9	PTF	TA, EDL, PL
10	FLFH	TP, PB, FDL, FHL

Table 5: Contents of the Ten Muscle Groups. Based on He et al. (1991)